Regular Article

An Autonomous Uncrewed Aircraft System Performing Targeted Atmospheric Observation for Cloud Seeding Operations

C. Alexander Hirst[1], John Bird[2], Roelof Burger[3], Henno Havenga[3], Gerhardt Botha[3], Darrel Baumgardner[4], Tom DeFelice[1], Duncan Axisa[5] and Eric Frew[1]

[1]Smead Aerospace Engineering Sciences, University of Colorado Boulder
[2]Aerospace and Mechanical Engineering, University of Texas at El Paso
[3]Unit for Environmental Sciences and Management, North West University
[4]Droplet Measurement Technologies, LLC
[5]Center for Western Weather and Water Extremes (CW3E), Scripps Institution of Oceanography, University of California San Diego

Abstract: This paper presents the results of a 3-week-long field deployment of an autonomous uncrewed aircraft system for targeted observation of early-convective storm systems in the U.S. Great Plains with application to cloud seeding operations. Due to reduced operational costs and requirements, autonomous small uncrewed aircraft systems present an appealing alternative to traditional crewed aircraft. The objective of the system is to gather and ultimately act upon in situ atmospheric data that are inaccessible via remote sensing techniques. Utilizing a combination of remote and in situ weather data, a dispersed autonomous decision-making system works integrally with a human operator to investigate early-convective storms for subregions which have favorable conditions for cloud seeding. The autonomy framework enables one operator to interface with multiple aircraft, which is demonstrated by performing complex sensing and seeding maneuvers with a team of two aircraft. Results from nine flights totaling over 8 hours of flight time are presented and discussed. Although the release of actual cloud seeding material was not performed during the campaign, this study demonstrates the utility and feasibility of small uncrewed aircraft systems for use in airborne cloud seeding operations.

Keywords: aerial robotics, environmental monitoring, rain enhancement

1. Introduction

With advancement in hardware, control, and sensing technologies, small uncrewed aircraft systems (sUAS) are increasingly deployed in a variety of remote and in situ sensing applications

Received: 15 December 2021; revised: 2 November 2022; accepted: 14 April 2023; published: 10 May 2023.

Correspondence: C. Alexander Hirst, Smead Aerospace Engineering Sciences, University of Colorado Boulder, Email: camron.hirst@colorado.edu

DOI: https://doi.org/10.55417/fr.2023022

(Elston et al., 2011b; Tang and Shao, 2015; Keating et al., 2016; Frew et al., 2020a). Small uncrewed aircraft have the advantage of being lower cost, easier to operate, and faster to deploy than crewed aircraft. Compared to more passive forms of traditional in situ sensing, such as towers and balloons, small uncrewed aircraft can be intelligently and actively controlled to take measurements at specific locations and times. This *targeted observation* ability makes sUAS especially suitable for in situ measurement of dynamic atmospheric phenomena.

Targeted observations by sUAS have exciting implications in a variety of fields. For example, teams of uncrewed aircraft have been deployed to take coordinated, targeted in situ measurements of supercell thunderstorm features, which would otherwise be inaccessible by crewed aircraft and are unmeasurable by remote sensors (Elston et al., 2011b; Frew et al., 2020a). These aircraft teams were loosely coordinated via assigning each aircraft a target region of large, developed storms to gather pressure, temperature, humidity, and wind data. A variety of complementary air and ground-based sensors simultaneously took measurements, all targeting the same storm in coordination. Ultimately, the sUAS measurements are to be fused with traditional sensors and assimilated into numerical weather prediction algorithms for improved severe storm forecasting (Jensen et al., 2021). Additionally, sUAS can be used for forestry management, as they can survey large swaths of land safer and cheaper than traditional methods (Tang and Shao, 2015) and for wildfire plume tracking, a dangerous but necessary task to provide situational awareness to first responders (Keating et al., 2016).

Targeted observations of the atmosphere also have the potential to improve autonomous sUAS capabilities. Future UAS traffic management concepts envision online weather forecasting at the scales that impact small UAS flight control (Prevot et al., 2016; Whitley, 2020). Characterizing weather hazards using data from small UAS will be an important aspect of this future system (Roseman and Argrow, 2020). Furthermore, closed-loop static (Depenbusch et al., 2018a; Depenbusch et al., 2018b) and dynamic (Bird et al., 2014; Silva and Frew, 2016) soaring have been demonstrated on sUAS with limited computational budgets. By actively sensing, modeling, and exploiting structures in the atmosphere, soaring has the potential to significantly increase sUAS endurance.

Uncrewed aircraft systems with lightweight state-of-the-art payloads (Figures 1 and 5) can measure meteorological state parameters, wind, aerosol, and cloud microphysical properties in

Figure 1. View from the Super RAAVEN uncrewed aircraft of an oncoming cloud. The miniaturized cloud droplet probe (CDP, top), multihole inertial probe (MIP, middle), and inlet to the portable optical particle spectrometer (POPS, bottom) are visible on the nose of the aircraft.

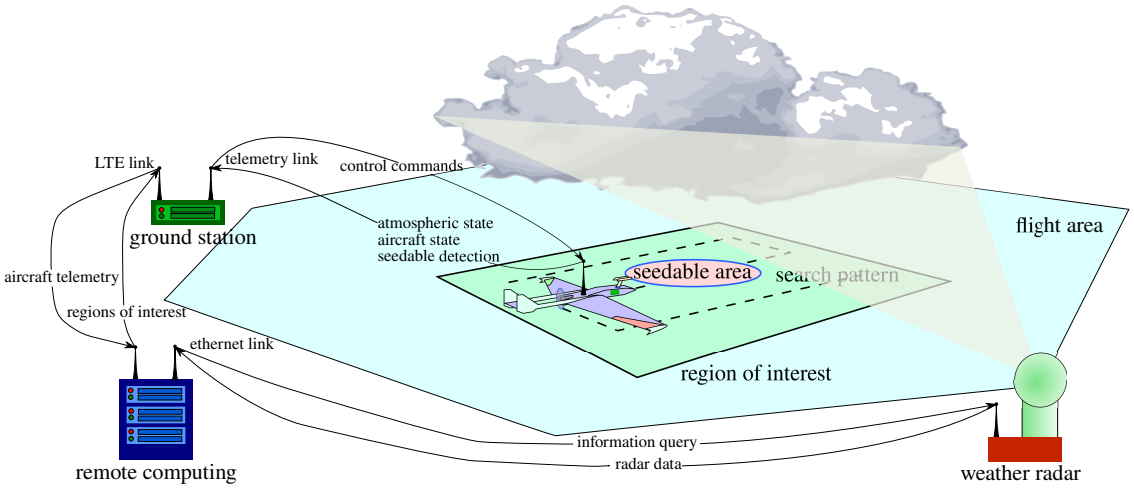

Figure 2. A high-level schematic of the demonstrated autonomous small uncrewed aircraft system for targeted rain enhancement. The system consists of a suite of complimentary autonomy algorithms run on a dispersed computational infrastructure (Section 4). Weather radar provides information for identification of regions of interest which are searched for seedable regions of the storm by a sensing aircraft.

conditions that are conducive to rain enhancement operations (Axisa and DeFelice, 2016; DeFelice and Axisa, 2016; DeFelice and Axisa, 2017), i.e., cloud seeding. Flight performance of sUAS has increased dramatically over the past decade, especially with improvements in autonomous control. Combined with the fast deployment times, low operational costs, and the ability to coordinate multiple aircraft in close proximity, sUAS present an appealing alternative to traditional manned airborne cloud seeding operations. These advantages are further multiplied in water-stressed regions with limited infrastructure for crewed aircraft operations.

This paper presents an sUAS (Figure 2) designed to take targeted in situ measurements of early-convective storm cells and conduct autonomous decision making for rain enhancement activities. The overall objective is to identify "seedable" regions of the atmosphere which are deemed suitable for cloud seeding operations. These regions are generally characterized by airborne moisture, particulate matter, and wind updrafts. Seedable regions are classified as microscale atmospheric features, meaning they exist on the order of hundreds of meters in size and time period on the order of minutes (Orlanski, 1975). The fast timescales and compact size of the targeted atmospheric features require rapid response to identified seedable regions for cloud seeding operations. Furthermore, due to payload restrictions, multiple small uncrewed aircraft must be deployed and tightly coordinated to make autonomous cloud seeding with sUAS a viable strategy. This unique challenge and application differentiates this work from other single aircraft (Elston et al., 2011b; Verdu et al., 2020) and loosely coordinated multi-aircraft (Frew et al., 2020a; Hattenberger et al., 2022) deployments for targeted atmospheric observation of convective storms.

To narrow the search space, real-time radar data are leveraged by a customized storm tracking algorithm to define regions of interest (ROIs), which are then searched by the sUAS for seedable regions using onboard sensing. Mapping of atmospheric features is not necessary, as the timescales of the targetable features are too short. The system is designed to conduct both single- and multi-aircraft missions, all through a single interface built to maximize the operator effectiveness and situational awareness of the environment and autonomy. It should be noted that actual cloud seeding was not conducted, meaning no seeding material was released during this campaign, as the focus of the work is validation of the autonomous system for targeted observation and aircraft coordination.

The contributions of the presented work are as follows:

- A dispersed autonomy architecture for targeted observation and in situ detection of meteorologically relevant features for cloud seeding operations.

- A task coordination state machine with supporting path planning for a team of two uncrewed aircraft performing targeted observation and seeding.
- Implementation of the proposed concept, with results of a 3-week field campaign in the Great Plains region of the United States. The field campaign demonstrates autonomous targeted observation of multiple storm cells by sensor-driven coordination of two small uncrewed aircraft.

The paper is outlined as follows: Section 2 discusses the concept of operations of the overarching targeted atmospheric observation mission. Section 3 describes the field-deployable hardware and software systems in depth. Section 4 provides details on the algorithms driving the dispersed autonomous system. Section 5 presents the objectives and results of the field campaign, with details on two particularly successful flight days. Section 6 presents a discussion on our keys to success and lessons learned from the 3-week field campaign in the U.S. Great Plains.

2. Concept of Operations

As the motivation for our system is rain enhancement via cloud seeding, flight operations will take place in the vicinity of clouds or thunderstorms that have already formed and possibly started to produce rain. The process of cloud seeding is intended to induce additional precipitation in the portions of the cloud that already contain sufficient moisture and would benefit from supplementary particulate matter to trigger microphysical processes that accelerate the formation of raindrops. Although conditions for cloud formation and rainfall can be forecasted in the U.S. Great Plains, they are not so understood and consistent that stationary operations are likely to provide a significant number of observation periods within a reasonably sized operational domain for an sUAS. Therefore, a mobile concept of operations was developed whereby the flight crew repositioned itself in response to the evolving weather conditions. Once a suitable site was located, flight operations were conducted by a stationary flight crew. Details of the concept of operations (CONOPS) are driven by two main factors: i.) the microphysics of cloud formation and precipitation, and ii.) aviation regulations for sUAS.

2.1. Cloud Microphysics

Cloud microphysics and seeding methodology dictate which regions of the atmosphere are suitable for cloud seeding. Historical macroscopic patterns and remote sensing make coarse forecasts of seedable regions possible, but not with enough precision in time or space to target release of seeding material from an aircraft. Seedable regions are dependent on microscale variations in environmental conditions, and seeding is most effective in convective systems prior to their evolution into large, highly convective, well-developed storms (Andreae and Rosenfeld, 2008). In situ observations can locate these phenomena and enable targeted dispersal of seeding material.

Targeting is often the most challenging part of operational cloud seeding programs. Current conceptual models of the seeding effect mostly presume that the seeding material makes it to the appropriate place at the right time. In this work, the hygroscopic seeding methodology is assumed, which triggers the warm rain process to enhance precipitation within clouds (Rosenfeld et al., 2010). This method of seeding introduces hygroscopic particles (salts) which readily take on water by vapor deposition in a supersaturated cloudy environment. During traditional seeding operations with crewed aircraft the salt particles are released into the base of convective clouds (e.g., Figure 3). These particles grow by vapor deposition and readily reach sizes that are large enough to initiate or participate in rain formation in the warm part of the cloud.

Based on this established cloud-seeding methodology and the underlying microphysical processes, the cloud seeding material should be released at a time and location i.) which is close to cloud bases that are sufficiently warm and where the warm rain process is marginally active, ii.) which is in an updraft area with vertical velocity large enough to carry seed particles up through the cloud bases, and iii.) where the concentration of cloud droplet forming aerosols is insufficient to lead to

Figure 3. A well-developed storm observed on August 19, 2021. The objective of our autonomous targeted observation system is to identify subregions in early-convective cells that would produce enhanced rainfall from cloud seeding operations.

rain formation. The challenge is to identify these cloud features via in situ observations and then deliver the seeding material in a timely manner.

Autonomously localizing seedable regions requires a hierarchical sensing approach which combines analysis from climatology, remote sensing, and in situ observation. Climatology can inform the flight team in advance of a deployment of general locations and seasons in which seedable clouds form. Local, public radar data such as the U.S. WSR-88D NEXRAD radar can be used to identify and track clouds as they form and develop, and can be used online to inform autonomous targeted observation systems. Finally, sensors onboard the sUAS are needed to measure the in situ cloud microphysical conditions to determine whether or not the local environment is suitable for cloud seeding.

2.2. Regulatory Requirements

The field campaign adhered to all relevant Federal Aviation Administration (FAA) regulatory requirements (Davis, 2008; Elston et al., 2011a) for public uncrewed aircraft operations. Flights were conducted under Certificate of Authorization (COA) 2020-WSA-5155-COA issued by the FAA to the University of Colorado Boulder.[1] This COA places restrictions on the scale of operations that can be conducted. These restrictions are in place to ensure that the sUAS operators can "sense and avoid" other air traffic (Davis, 2008; Elston et al., 2011a).

[1] https://www.colorado.edu/isc/flight-operations/current-cu-owned-coas

The relevant restrictions include the following:

- The flight crew must have a minimum of two crew members: i.) the pilot-in-command who has final authority and responsibility for the operation and safety of the flight, and ii.) a visual observer who assists the pilot-in-command and the person manipulating the flight controls to see and avoid other air traffic or objects aloft or on the ground.
- Flight operations must end no later than 30 minutes after local sunset.
- The aircraft is limited to an altitude of 2500 ft (762 m) above ground level (AGL).
- The aircraft must remain within 1.0 miles (1.61 km) laterally from the flight crew.
- The aircraft can only operate in visual meteorological conditions in which visual flight rules are followed, which effectively means the aircraft must stay 500 ft (152.4 m) below the cloud ceiling.
- A notice to air missions (NOTAM) that specifies the flight location must be issued 1 hour in advance. Aircraft operation must be within 10 miles (16.09 km) of the reported location.

2.3. Single-aircraft and Multi-aircraft Autonomous Targeted Observation and Seeding

Two similar concepts of operations (CONOPS) were developed for single-aircraft and multi-aircraft missions. In both missions the initial stages of the CONOPS are the same. The initial stage of the CONOPS begins the day before operation when weather forecasts by collaborating meteorologists are used by an in-field meteorologist to determine the likelihood of favorable conditions occurring over the next 36 hours, the general location of these favorable conditions, and a location for operation the next day in order to determine the overnight staging location. On the day of operation, local weather forecasting is again used to identify a preliminary operational area. Since cloud formation in the U.S. Great Plains typically occurs in the midafternoon and evolves over several hours, this preliminary operational area can encompass hundreds of square miles up to several hours drive from the team's overnight staging location. As the flight team moves toward the operational area through the morning and early afternoon, nowcasting is performed by the in-field team meteorologist to refine the location and size of the operational area.

The flight operation area is jointly determined by the in-field meteorologist and flight crew to be admissible for aircraft operations and within the likely path of a potentially seedable storm. Storms may or may not have formed before the operation area is determined, but forecasts and domain expertise aide in the decision-making process. Once the location is determined, it takes approximately 30 minutes to prepare the aircraft for launch. Preparations include assembling the modular airframe, setting up the bungee launch system, and installing batteries into the aircraft. The preparation delay is fairly significant for the timescales of targeted atmospheric phenomena, making accurate forecasting and nowcasting by the in-field meteorologist crucial for mission success. Once prepared, premission checks are made of the onboard sensors and software, and the sUAS is launched and then transitioned to autonomous mode by the operator. The mission can be conducted fully autonomously, though the human operator has the ability to manually intervene to manipulate or disable the autonomy stack (Section 4) which controls the aircraft.

This work formulates a primary multi-aircraft CONOPS with two uncrewed aircraft (UA). Size and weight considerations require multiple aircraft be deployed for realistic rain enhancement operations from sUAS. One aircraft, referred to as the *Sensing UA*, carries the sensors which identify a point within seedable regions called a *seeding location* at which to trigger the release of cloud seeding material. The other aircraft, called the *Seeding UA*, carries the seeding material and deployment system. This division of tasks also enables measurement of the cloud environment to occur at the same time as material dispersal by positioning sensors downwind of the seeding location. A targeted release of seeding material at a seeding location therefore requires coordination between the two aircraft, which is achieved through the multi-aircraft finite state machine described in Section 4.4. While less realistic, a secondary single-aircraft CONOPS was also developed as a complexity stepping stone to the multi-aircraft mission. The single-aircraft mission consists of a single uncrewed aircraft preforming both Sensing UA and Seeding UA functions. See Section 4.3

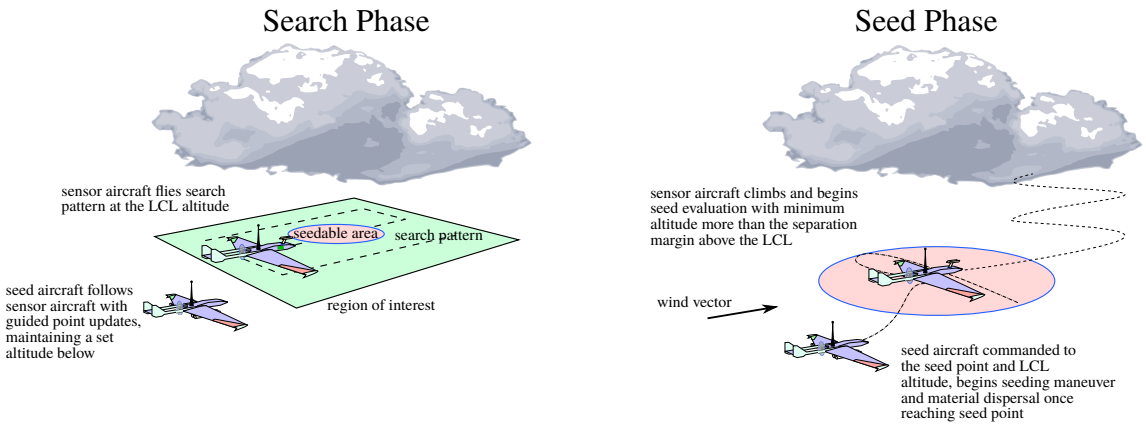

Figure 4. Multi-aircraft coordination for targeted rain enhancement. A sensing vehicle identifies regions suitable for seeding while a seeding vehicle carries the material and dispersal system. This allows the sensing vehicle to maneuver to assess the impact of the material on the cloud environment during seeding operations.

for a description of the single-aircraft finite state machine implementation. **Note, the Seeding UA in both the single- and multi-aircraft missions described and deployed in this paper did not carry seeding material, however the autonomy system was developed and performed as if it did by carrying out a virtualized seeding task when appropriate**.

Both the single- and multi-aircraft autonomous missions consist of three main phases: *Loiter*, *Search*, and *Seed* (Figure 4). During the *Loiter* phase the aircraft maintains a holding pattern while the Rapid Evaluation of Convective Cell Environments for Seeding (RECCES) algorithm (Section 4.1) uses WSR 88-D NEXRAD weather data to monitor the growth of storms, track their movement, and report a region of interest (ROI) to the sUAS. Once an ROI has been identified and provided to the sUAS, it transitions to the *Search* phase. During this phase, the Sensing UA follows a search path that covers the ROI while it monitors for seedable regions by calculating a seedability score (Section 4.2) from in situ measurements. For the multi-aircraft mission, the second Seeding UA trails behind the Sensing UA in loose formation. This phase ends when the Sensing UA identifies an area from in situ conditions suitable for seeding.

The final *Seeding* phase coordinates multiple maneuvers and aircraft. In the experiments described in Section 5 the seeding event itself is virtualized, i.e., the aircraft performs the realistic seeding maneuver but does not actually release any material. However, all other decisions and actions occur as if it had. For the single-aircraft mission, upon identifying a seedable location the aircraft immediately performs the seeding maneuver and then transitions to an evaluation maneuver to circle back into the area where the seeding occurred. For the multi-aircraft mission, the Sensing UA communicates the seedable location to the Seeding UA, which immediately maneuvers to the seedable location to conduct a seeding maneuver. At the same time, the Sensing UA initiates the evaluation maneuver downwind of the seeding location to measure atmospheric changes. Evaluation maneuvers are intended to position the Sensing UA such that it can measure any changes in atmospheric conditions via the onboard sensors (Section 3.1.1) that may be triggered by releasing seeding material from the Seeding UA. This aircraft-to-aircraft coordination is achieved via planning and control algorithms run on an in-field ground control station. Details on these maneuvers and the autonomy finite state machines are provided in Sections 4.3 and 4.4.

3. System Overview

3.1. Sensing Aircraft: Super RAAVEN

The primary aircraft, the Sensing UA, in this system is the Super Robust Autonomous Aerial Vehicle - Endurant and Nimble (Super RAAVEN, Figure 5). A descendent of the original RAAVEN

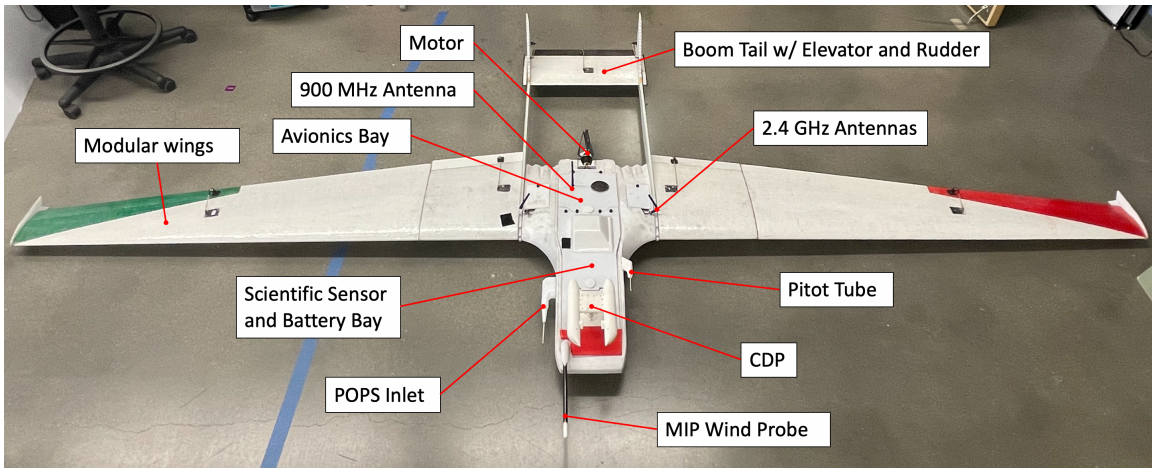

Figure 5. The Super RAAVEN uncrewed aircraft used for the targeted observation of early-convective storm systems.

aircraft, which has seen consistent success in various data collection deployments (Frew et al., 2020a; de Boer et al., 2021), the Super RAAVEN was designed and built by the University of Colorado Boulder Integrated Remote and In Situ Sensing (IRISS) team, in collaboration with Rite-Wing RC. The Super RAAVEN has enhanced payload and endurance capabilities, allowing it to carry the relatively large onboard sensor suite required for cloud seeding missions. The Super RAAVEN airframe is molded from the same EPP foam as the RAAVEN, with carbon fiber and aluminum spars providing structural support to enable the extended wingspan of 4.19 m. The aircraft is powered by two 21,000 mAh batteries and one 10,500 mAh lithium-ion battery. With a gross takeoff weight of 13.6 kg and a cruise speed of 16 m/s, the Super RAAVEN has up to 2 hours of endurance with the sensor suite flown in the campaign. The Super RAAVEN payload consists of three scientific sensors, flight sensors, avionics, a BeagleBone Green companion computer, and two radios.

3.1.1. Scientific Sensor Payload

The scientific sensor payload consists of three sensors, the Handix Scientific Portable Optical Particle Spectrometer (POPS),[2] the Droplet Measurement Technologies Cloud Droplet Probe (CDP),[3] and the Rain Dynamics Miniature Inertial Probe (MIP).[4] The POPS provides atmospheric particulate matter size and concentration measurements, necessary for quantifying cloud condensation nuclei (CCN) concentration. The CDP measures size and concentration of water droplets in the atmosphere. The MIP provides aircraft state, three-dimensional wind velocity vector, temperature, humidity, and atmospheric pressure. Combined, these sensors inform an onboard, online cloud seedability algorithm (CSA), which provides succinct information about the current atmospheric state by way of a seed score, seed/no seed decision, and the Liquid Condensation Level (LCL) altitude and temperature (Section 4.2). These sensors can also be used to detect changes in water droplet and CCN concentrations induced by seeding during evaluation maneuvers performed by the Sensing UA.

The MIP and CDP are purpose-built sUAS versions of larger and heavier sensors traditionally flown on cloud seeding crewed aircraft, while the POPS was flown in its default configuration. An onboard BeagleBone Green companion computer equipped with a custom-printed circuit board cape interfaces with all scientific sensors, logs data, runs the CSA and transmits relevant data to the ground over a serial radio via the autopilot MAVLink connection.

[2] http://www.handixscientific.com/pops
[3] https://www.dropletmeasurement.com/product/cloud-droplet-probe/
[4] Website unavailable at time of writing.

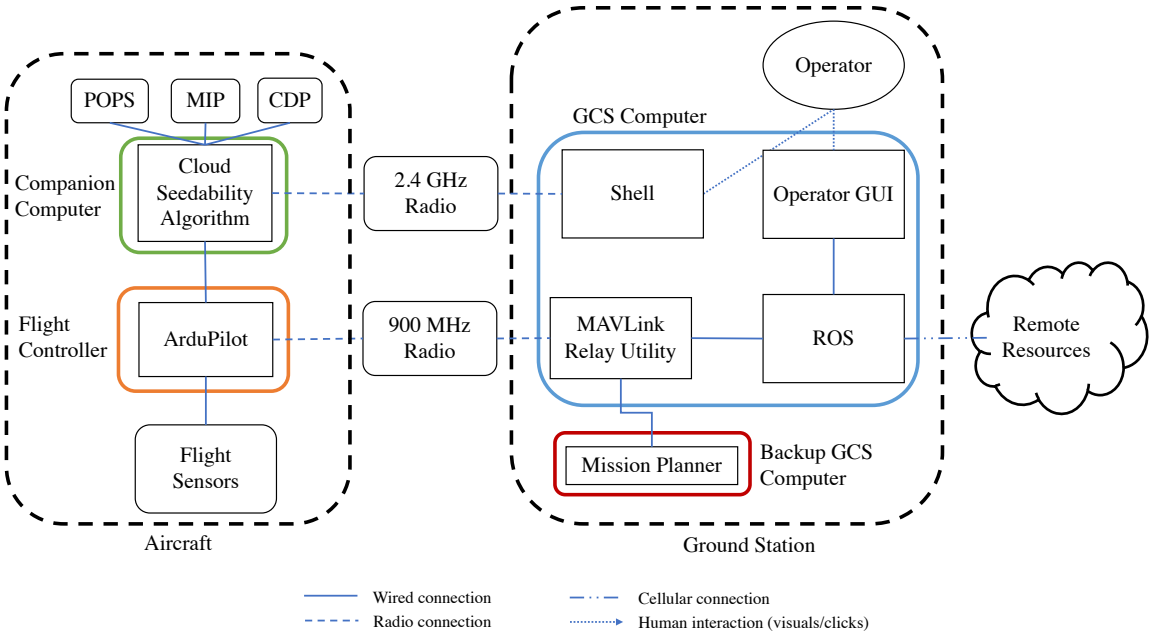

Figure 6. Schematic diagram of the in-field communication and computation infrastructure. Square boxes represent software modules while rounded boxes represent hardware components. In-field computers are color-coded to demonstrate the dispersion of autonomy algorithms across multiple platforms in the field. The multi-aircraft mission requires an additional 900 MHz radio for command and control of the Seeding UA. The Seeding UA payload consists of only the flight controller and flight sensors.

3.1.2. Avionics, Flight Sensors, and Radio Payload

The aircraft is controlled by an onboard Hex Cube Black Flight Controller running ArduPilot, an open-source autopilot firmware (ArduPilot, 2019). Localization and state estimation is provided by an integrated magnetometer, accelerometer, and the HEX Here GPS module. Airspeed measurements are taken with a Matek System ASPD-4525 airspeed sensor. The autopilot communicates with the ground station via a MicroHard 900 MHz serial radio using the MAVLink protocol, providing aircraft state and scientific data at approximately 1 Hz. In turn, the ground station provides aircraft guidance commands via the same serial radio connection at a rate of 2 Hz. The guidance commands are simple 3D positions which are generated by behavior nodes in the finite state machine (Sections 4.3 and 4.4). A direct connection from the ground station to the companion computer is provided by a MicroHard 2.4 GHz Ethernet radio; this link is used via a shell session for configuring the sensor interfaces, data logging, and CSA software before flight. Figure 6 depicts the in-field communication and computation architecture used during the deployment. The in-field architecture is a subset of the complete dispersed autonomy architecture discussed in Section 4.

3.2. Seeding Aircraft: RAAVEN

During this campaign, the secondary seeding aircraft (Seeding UA) was a RAAVEN (Figure 7) in its standard configuration (Frew et al., 2020a). The payload consists only of avionics and flight sensors; no scientific sensors were onboard. The avionics and flight sensors are identical to the Super RAAVEN. The RAAVEN is used for its durability and quick launch capability. As this field campaign did not require dispersal of seeding material, an aircraft with larger payload capacity was not required. The Seeding UA is controlled and coordinated via an additional 900 MHz radio using the MAVLink protocol. Guidance commands via simple 3D positions are generated by behavior nodes in the Sensing UA finite state machine (Section 4.3) to realize the desired behaviors.

Figure 7. The RAAVEN uncrewed aircraft system, which acts as the Seeding UA for this work.

Figure 8. Ground vehicles used to transport all flight and computer gear required for single and multi-aircraft missions.

3.3. Nomadic Ground Station

All crew members and equipment required to fly the single- and multi-aircraft missions were transported in two SUVs (Figure 8). This configuration allows for nomadic operations, which were required to find and intercept a suitable number of storm cells in the U.S. Great Plains. All ground station hardware and electronics were located in a single vehicle, which was also outfitted with GPS and an operator workstation (Figure 9). Consistent cellular connection in the U.S. Great Plains allows for reliable connection to an in-house built remote server. Live sUAS and weather data were published and visualized on a Mission Observation Graphical Interface served by this remote server for increased situational awareness and communication between local and remote team members. The remote server also hosted a message passing service which enabled dispersed components of the autonomy architecture to communicate. Dispersed computational infrastructure for sUAS control was first demonstrated in severe storm operations (Frew et al., 2020a). Finally, a secondary ground station control computer running ArduPilot Mission Planner was utilized during all flights to aid in aircraft startup and provide redundancy in case of autonomy system failure.

4. Dispersed Autonomy Architecture

This section presents the decision-making algorithms which drive the autonomous aircraft system for both single- and multi-aircraft missions. The autonomy architecture is dispersed (Frew et al.,

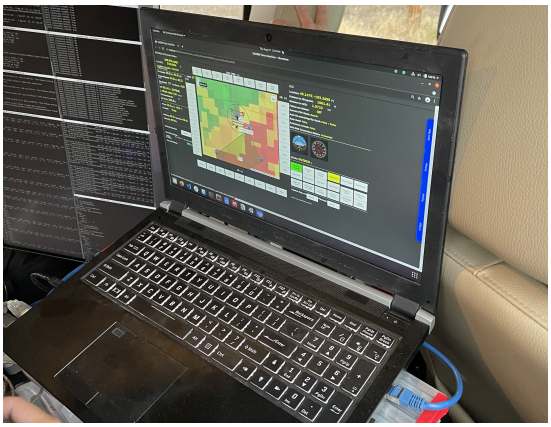

Figure 9. The ground control station configured in the nomadic ground vehicles.

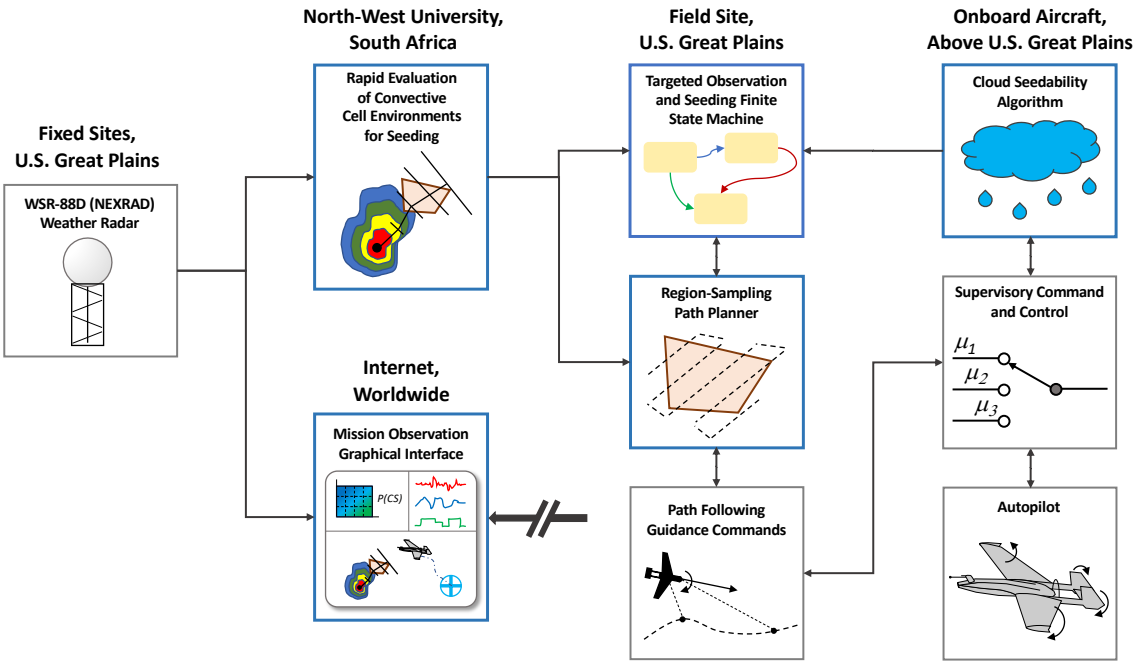

Figure 10. Autonomy is achieved through a dispersed architecture that includes components run on remote computing resources, on the fielded ground station, onboard the aircraft, and served through a web browser. The main components developed for this targeted observation and seeding system are indicated by the heavy-lined blue boxes. The labels above the boxes state the location of the computer implementing the algorithms. The arrows indicate the main direction of information flow with all component feeding information to the Mission Observation GUI. Not depicted is the fact that aircraft state information is available to all components.

2020b), meaning it makes use of remote, edge, and onboard computing resources to control the system (Figure 10). Doing so takes advantage of modern communication networks to reduce online resources required in the field, while simultaneously enabling complex decision-making algorithms.

There are five main components of the dispersed autonomy architecture: (i) the Rapid Evaluation of Convective Cell Environments for Seeding (RECCES) algorithm; (ii) the cloud seedability algorithm (CSA); (iii) finite state machines that coordinate aircraft actions; (iv) a path planner for sampling regions of interest identified by RECCES; and (v) the human-robot interaction and

enabling graphical user interfaces. These components are run on cloud computing resources, onboard the aircraft, on the fielded ground station, and served through a web browser.

4.1. Radar and the RECCES Algorithm

The Rapid Evaluation of Convective Cell Environments for Seeding (RECCES) algorithm was developed to define regions of interest (ROI) where seedable conditions are likely to occur over time and space. These ROIs thus define a reduced search space that is tractable for an sUAS to survey as the atmospheric features evolve. RECCES uses near real-time observation to predict where these potential areas could be and chooses optimal ROIs based on mission objectives and constraints. The algorithm is implemented on a cloud-based server and connected to the in-field ground station via cellular communications (Figure 10).

RECCES uses multiple input data streams, including short-term forecasts, a convective storm climatology, satellite cloud products, weather radar, and the position of the Sensing UA and in-field ground station to identify an optimal ROI. Each of these streams provides complementary information that is useful for a variety of missions. Weather radar is used to observe convective cells that have produced precipitation-sized cloud drops. Weather radar data were streamed from the Cheyenne (KCYS), Denver (KFTG), Goodland (KGLD), and North Platte (KLNX) weather radars during the field deployment. The radar data are publicly available in real-time through the Amazon Web Service (NOAA, 2015). Satellite data from the advanced baseline imager (ABI) band 11 (at 8.5 μm) provide cloud brightness temperatures, and they are used to identify new cloud development which is not yet visible in radar echoes (NOAA, 2017). A convective forecast was made every morning by the meteorological team over a preferred region of operation. These forecasts contained input ROIs for RECCES that can be used when remote sensing data are unavailable. A convective climatology was also constructed from historical radar data and can also be used if observations of clouds or convective cells are not available at runtime. Lastly, aircraft state and ground station position information was streamed from the in-field ground station to identify admissible and prioritize ROIs. In situ measurements from the onboard sensors of the aircraft are not used as an input to RECCES.

The RECCES algorithm consists of several subroutines (Figure 11). First, RECCES continuously identifies and tracks four classes of cloud products (Table 1) from measurement data: (1) Developing Convective Cells, (2) (developed) Convective Cells, (3) Updraft Regions, and (4) New Cloud Development, using the Lidar Radar Open Source Environment (LROSE) (Heistermann et al.,

Table 1. RECCES algorithm cloud products and descriptors. These cloud products are used to define admissible ROIs to be investigated by the search aircraft. As Developing Convective Cells most often result in seedable conditions, these products were highest priority during deployment.

Cloud Product:	Developing Convective Cells	Convective Cells	Updraft Regions	New Cloud Development
Description:	Developing cumulus cells, observable via radar echoes	Developed, medium to small cumulus cells	Developing updraft regions in large, developed convective storms	New cloud development observed via satellite, before radar echoes.
Priority:	1 (highest)	2	3	4
Tracking Threshold:	18 dBz	30 dBz	30 dBz	N/A
Tracking Method:	TITAN Cells	TITAN Cells	Weak echo regions	All pixels
Minimum Height:	3 km	0 km	N/A	N/A
Maximum Height:	8 km	20 km	N/A	N/A
Forecast Horizon:	15 min	30 min	5 min	15 min
Forecast Type:	Linear Trend	Parabolic Trend	Static	Linear Trend
Initial Movement:	Optical Flow Field	Optical Flow Field	N/A	Optical Flow Field

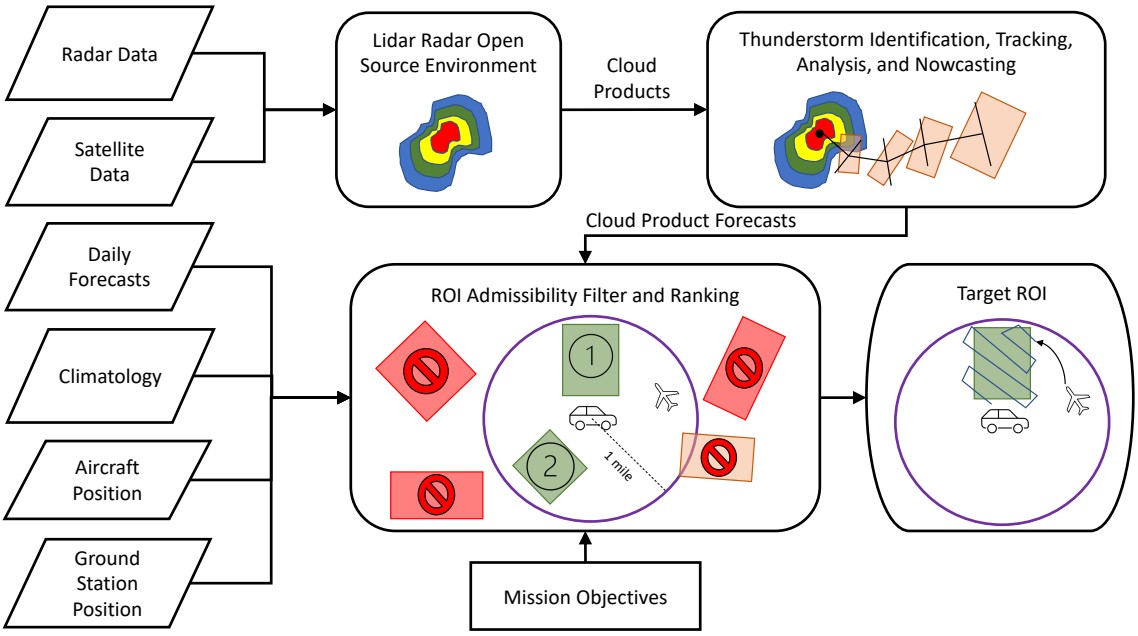

Figure 11. An information flow diagram for the Rapid Evaluation of Convective Cell Environments for Seeding (RECCES) algorithm. Satellite and radar data are streamed in real-time for use in RECCES. Convective climatology and daily forecasts are conducted offline, but may be used online if real-time data streams are insufficient for defining an ROI. Scientific and robotic data inputs are shown as parallelograms, while internal RECCES modules are rounded rectangles. Mission objectives can be changed online by an operator to target different cloud products. The output of RECCES is a single target ROI for the fielded uncrewed aircraft to search.

2015). Each cloud product serves as a proxy for developing areas in convective storms, and ROIs targeting each product class are nominally ranked based on the expected likelihood of encountering seedable regions of the atmosphere.

After identification, future positions of cloud products are predicted in three steps. First, the spatial scale of features is determined to correctly match the relevant time frame for which realistic now-casts can be made (Dixon and Seed, 2014). Second, flow fields are estimated using an optical tracker to predict the movement of smaller scale products. Finally, RECCES uses the Thunderstorm Identification, Tracking and Analysis (TITAN) algorithm to identify the positions of products and predict their movement using linear or parabolic trend relationships (Dixon and Wiener, 1993). Larger scale products, such as weak echo regions (aka Updraft Regions), are assumed to be static.

RECCES then fits a set of polygons which define the current and future locations of each cloud product in 1-minute time increments over a discretized time horizon (Figure 12). Polygons are also fitted to preferred and admissible regions of operation, based on the current aircraft and ground station positions. Finally, RECCES uses specific mission objectives and constraints to select and scale a single admissible ROI polygon, and then communicates this ROI to the autonomy system. In the presented field deployment, the single ROI was chosen to be rectangular and reside fully within one mile of the current position of the in-field ground station while intercepting the highest priority, reachable cloud product (Figures 11 and 16). While more generic shapes and complex objective functions may have allowed for a more efficient search, rectangular ROIs simplified aircraft path planning and compliance with FAA restrictions. We note that cloud product priority rankings can be modified online based on the current mission objectives and constraints. For example, earlier atmospheric development can be favored by prioritizing ROIs targeting New Cloud Development products, while growing convective cells can be favored by prioritizing ROIs targeting Developing Convective Cells or Convective Cells.

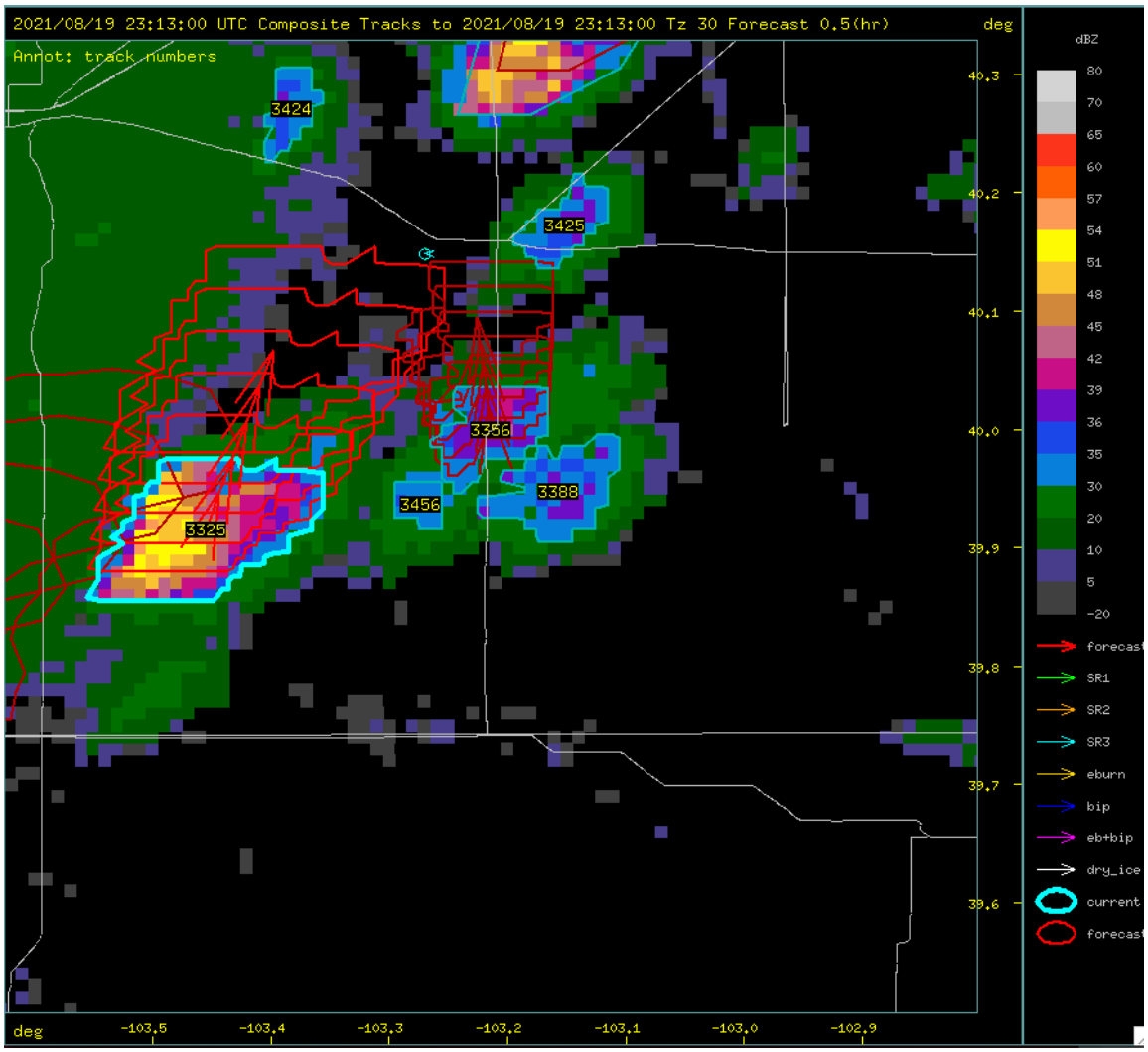

Figure 12. A visualization of the RECCES algorithm before Flight #5 on August 19, 2021. The convective storms are outlined with a bolded light blue line, while forecasted storm evolution is shown in red. The location of the Seeding UA is shown as a light blue arrow. The Sensing UA is in the forecasted path of storm evolution.

The RECCES algorithm can be tuned at the storm identification, scale analysis, and nowcasting stage. Best-guess parameters were implemented and tuned throughout the field campaign. One of the most important and challenging tuning parameters is the time offset between the actual observation time and the reported observation time. The radar and satellite sensors obtain their scan over a prolonged time period, which was empirically determined to be 10 minutes for both sensors during the campaign. While the movement of storms during the scan period is normally ignored, it became important when matching the position of the aircraft with the position of the candidate ROIs.

4.2. Cloud Seedability Algorithm

Running onboard the Sensing UA, the cloud seedability algorithm (CSA) identifies, in real time, regions where seeding will have the highest probability of accelerating the formation of drizzle, from which rain forms, and the lowest probability of having the opposite effect, i.e., suppressing precipitation. The algorithm incorporates a model that simulates how cloud droplets form from

Table 2. Cloud seeding algorithm variable definitions and nominal ranges.

Parameter Name:	Parameter Description:	Nominal Range:
T_{base}	Cloud base temperature	5 °C – 30 °C
w	Updraft velocity	0.1 – 20 m/s
N_{CCN}	Concentration of cloud condensation nuclei	100 – 1000 cm^{-3}
$\Delta t_{seed}(T_{base}, w, N_{CCN})$	After seeding at cloud base, the number of seconds for drizzle to form for a constant updraft and CCN concentration	0 – 100 s
$\Delta t_{no-seed}(T_{base}, w, N_{CCN})$	With no seeding at cloud base, the number of seconds for drizzle to form for a constant updraft and CCN concentration	0 – 100 s

cloud condensation nuclei (CCN) and then subsequently grow by condensation and coalescence. The formation and evolution of cloud droplets has been studied for years, and many models have been developed and validated that simulate the microphysical and dynamical processes of convective clouds. The CSA is based on these studies and uses what is known as a parcel model (Howell, 1949) whereby a volume of air rises in an updraft and cools adiabatically until the environment becomes supersaturated, i.e., when the relative humidity exceeds 100%. The rate at which cloud droplets form and grow depends upon the temperature of the cloud base, T_{base}, the speed at which the air rises, w, and the concentration of the CCN, N_{CCN}.

Given the unavailability of information on the size or composition of the CCN in the United Arab Emirates, which is the region for which the sUAS presented here was designed, the alternative was to evaluate measurements of the CCN concentrations that were made with an instrumented aircraft in September 2017 (Orikasa et al., 2020) and shared via personal communication. An analysis of 14 flights provided not only an extensive database of CCN measurements, but also information on the vertical profiles of temperature, humidity, and updraft over a wide range of cloud base conditions. The cloud base temperatures ranged from 5 to 25 °C, updrafts from 0.1 to 10 ms^{-1}, and CCN concentrations from 100 to 1000 cm^{-3}.

The objective of the CSA is to determine how adding extra CCN (seed material) at cloud base will change the time it takes to develop precipitation. It is assumed that the probability of enhancing precipitation is inversely proportional to the time Δt_{seed} from when the seed material is introduced to when the first precipitation drops appear. The strategy for estimating this probability was to run the model over many sets of T_{base}, w, and N_{CCN}, covering the whole range of values that were measured (Orikasa et al., 2020). The model was run for each set of conditions until the time $\Delta t_{no-seed}$ when 100 μm drops appeared, which are considered precipitation-size droplets. The model was then run over the same conditions, but with increased N_{CCN} by 500 cm^{-3} over nominal, the estimated change in CNN concentration due to releasing seeding material. The time Δt_{seed} to reach 100 μm was again determined using this new N_{CCN}. If $\Delta t_{seed}(T_{base}, w, N_{CCN}) < \Delta t_{no-seed}(T_{base}, w, N_{CCN})$, then the probability $P(seed|T_{base}, w, N_{CCN})$, that seeding will enhance the formation of precipitation at that atmospheric condition, will be greater than zero. CSA variable descriptions and nominal ranges can be found in Table 2.

The results from the thousands of model runs were converted into a *cloud seedability score* (css) that is normalized between 0 and 100 for each T_{base} by

$$css(T_{base}, w, N_{CCN}) = \begin{cases} 100 \times \frac{\Delta t^{min}_{seed}(T_{base})}{\Delta t_{seed}} & \text{if } \Delta t_{seed} \leq \Delta t_{no-seed}, \\ 0 & \text{otherwise,} \end{cases} \tag{1}$$

where $css(T_{base}, w, N_{CCN})$ is the score and

$$\Delta t^{min}_{seed}(T_{base}) = \min_{w, N_{CCN}} \Delta t_{seed}(T_{base}, w, N_{CCN}) \tag{2}$$

is derived in order to normalize the result. The cloud seedability score is proportional to $P(seed|T_{base}, w, N_{CCN})$ since

$$P(seed|T_{base}, w, N_{CCN}) \propto \frac{1}{\Delta t_{seed}(T_{base}, w, N_{CCN})} \propto css(T_{base}, w, N_{CCN}). \tag{3}$$

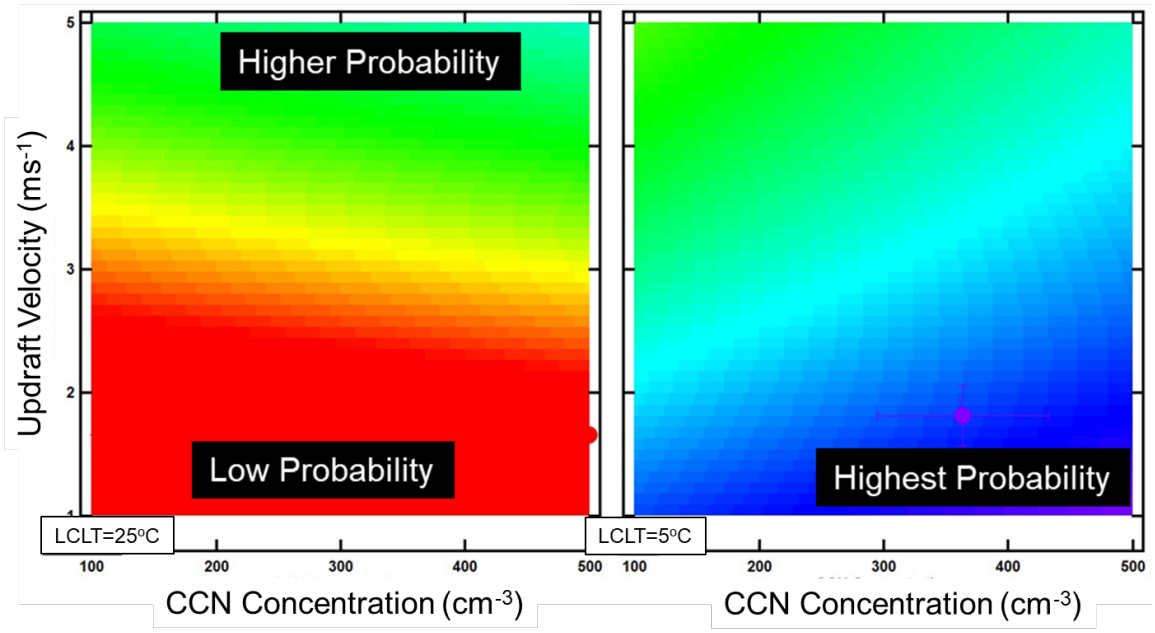

Figure 13. These two diagrams illustrate how the probability is dependent on the lifted condensation level (LCL), CCN concentration, and updraft velocity. When the LCL is warmer (left panel), the probability that seeding will be effective increases with increasing updraft, but at colder LCLs the opposite is the case (right panel).

The decision to initiate seeding is based on an empirical threshold $css(T_{base}, w, N_{CCN}) > css_0$ with a value of $css_0 = 50$ used for the experiments described in Section 5.

Figure 13 illustrates these scores as color maps where the cooler colors represent the highest probabilities and the warmer colors the lower probabilities. Note that on this figure is the acronym LCLT, which is short for Lifted Condensation Level Temperature. The LCLT is the temperature that is equal to the dew point temperature, i.e., the expected cloud base temperature. The LCLT is a standard parameter that is reported from atmospheric sounding measurements because it is the expected cloud base temperature given the vertical profile of pressure, temperature, and humidity. The LCLT is used here as an estimate of the temperature of the cloud base, i.e., $\hat{T}_{base} = LCLT$.

The probability maps for LCLTs from 5° to 25° in 1° increments were fit with a nonlinear function with w and N_{CCN} as the input variables. The regression coefficients are stored in a table that the CSA accesses in real time to compute $css(T_{base} = LCLT, w, N_{CCN})$.

Operationally, prior to launch the LCLT is found from the most recent and closest sounding. This LCLT determines which coefficients to use when computing the probabilities from the aircraft's measurements of w and N_{CCN}. Note that the aerosol measurements from the POPS are a surrogate for the CCN because the evaluation of the measurement data (Orikasa et al., 2020) showed a strong correlation between the ambient aerosol concentrations of particles larger than 0.2 μm, the lower threshold of the POPS, and N_{CCN}.

Once in flight, when the region of interest is reached, the CSA is continuously updated with the temperature, dew point, updraft velocity, and N_{CCN}. If the temperature is within one degree of the dew point temperature, the CSA recognizes this as a new LCLT and updates accordingly and also sends this altitude to the ground station as this is the best estimate of cloud base.

4.3. Single-Aircraft State Machine

A finite state machine coordinates the behaviors that enable targeted rain enhancement. A state is defined for each task in the rain enhancement process, and transitions between states are identified

Table 3. Single aircraft mission finite state machine states, transitions, and descriptions of states.

State:	Description:	Transitions to:	Transitions from:
Safe	Inert state, operator must manually activate the autonomy to transition out.	Loiter	Initialization, All states
Loiter	Reposition the aircraft, wait for ROIs to be identified.	Safe, Profile, Search, Seed	All states
Profile	Take vertical profiles of the atmosphere while orbiting the profile location.	Safe, Loiter	Loiter
Search	Fly a search pattern within an ROI, looking for seedable regions.	Safe, Loiter, Release Seed Material	Loiter
Release Seed Material	Fly seeding maneuver at seed point and altitude.	Safe, Loiter, Evaluate	Search
Evaluate	Fly an evaluation maneuver relative to the seed point.	Safe, Loiter	Release Seed Material

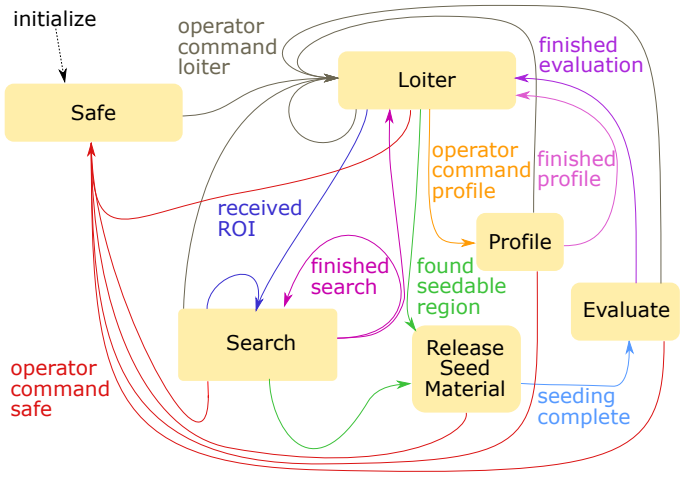

Figure 14. A diagram of the single aircraft finite state machine.

and associated with signals generated by the operator or autonomy system. Separate finite state machines are created for the single-aircraft and multi-aircraft missions, though they share most of the same states and transitions.

The single-aircraft mission consists of six distinct states (Figure 14), as outlined in Table 3. These states are Safe, Loiter, Profile, Search, Release Seed Material, and Evaluate. This is a subset of the states present in the multi-aircraft finite state machine. Both single- and multi-aircraft state machines are implemented using the Robot Operating System (ROS) (Quigley et al., 2009) and the `smach` package,[5] and they are run onboard the fielded ground station computer.

The finite state machine can be configured in real-time by the operator to request operator input at various transitions and phases of the CONOPS, thus setting the human operator either in-the-loop or on-the-loop. If configured appropriately, the autonomy stack can work fully autonomously end-to-end once activated. However, deployment demonstrated the utility of having a human operator integrated with the autonomy, as they are able to make high-level decisions and incorporate the latest semantic information provided by the in-field meteorologist.

The Safe state is the default state of the system at initialization. It provides an inert environment for repositioning and troubleshooting while the aircraft is flying. The Safe state prevents any

[5] http://wiki.ros.org/smach

autonomy-induced transition from occurring without explicit permission from the operator. The act of enabling transitions from Safe is referred to as *activating the autonomy*. While in the Safe state the operator is able to manually reposition the aircraft, set target altitudes, and configure various parts of the autonomy by issuing commands from the ground station computer.

The Loiter state is used to position the aircraft at a desired location while the autonomy system is active. The primary function of this state is to allow the operator to position the aircraft in the vicinity of expected regions of interest while awaiting an ROI from the RECCES algorithm. The Loiter state can also be used to position the aircraft in response to direction from the meteorological team in order to obtain in situ measurements of an interesting region.

In the Profile state the aircraft climbs above the expected Liquid Condensation Level (LCL) altitude in order to gather atmospheric measurements and calculate the current LCL altitude via the CSA. The LCL altitude is at the base of the clouds and is most favorable for dispersing material. The LCL altitude constantly changes due to temporal and mesoscale spatial variations in humidity. These variations make it undesirable to specify the aircraft operating altitude based on forecasts or preflight balloon soundings. Due to the altitude limitations imposed on the missions by the FAA, the deployed aircraft systems were unable to achieve LCL altitude during the campaign, thus this state was not used regularly in the field deployment. However, in future operations this state can be used to provide LCL altitude information for targeted observations of the cloud base.

The Search state searches the ROI for *seeding locations* which are point positions in space and are subsets of seedable regions. On receipt and approval (optionally by the human operator or internal checks) of an ROI, a search flight plan is computed which covers the ROI and the guidance system begins generating waypoint commands to fly the search pattern. ROIs can be provided either autonomously by the RECCES algorithm, or manually by the human operator. Manual ROIs were provided if RECCES was unavailable or was unable to find a suitable storm within the current operational area of the field crew. Several search patterns are available for selection by the operator. These include spiral in, spiral out, raster, and diagonal plans. The patterns were configurable within the GUI, but all assume a rectangular, arbitrarily rotated ROI. During the campaign the operator primarily used raster and diagonal patterns. The autonomy will fly the complete search path. If no seeding locations are flagged after flying the complete path, the system will either transition back to Loiter or re-search the ROI. This behavior is configured by the operator. If the system transitions back to Loiter without seeding, then the mission is completed and the system waits for a new ROI to be provided before initiating another search.

If in situ observations identify a region suitable for seeding, the associated location is flagged and the aircraft immediately transitions to the Release Seed Material state. In this state the aircraft flies a seeding path while (virtually) dispersing seeding material. The seeding path is designed to release material while the aircraft course angle is perpendicular to the current estimated horizontal wind vector. This maneuver is similar to how crewed aircraft release material. Again, note that while no seeding material was released during the presented field campaign, the system was developed and controlled as if it was.

Finally, the Evaluate state is designed to measure changes in the atmosphere during and after seeding material is released. In the single aircraft mission, this is performed sequentially after the Release Seed Material state. In this state the aircraft flies a path which sets the aircraft course tangent to the wind vector, while being directly downwind of the flagged seed point. This path would have enabled the aircraft to detect the impact of releasing seeding material on the cloud environment via the onboard sensors (Section 3.1.1) had seeding material been dispersed. Ideally, hydroscopic seeding would increase precipitous droplet concentration and cloud condensation nuclei, which are detectable by the CDP and POPS, respectively. Conclusion of the Evaluate state results in the system returning to Loiter, thus completing a mission. The autonomy then waits for a new ROI to be provided to search, although the operator is able to manually command a search of the previous ROI. Therefore, the autonomy assumes by default that only a single seeding maneuver should be conducted per ROI.

4.4. Multi-Aircraft State Machine

To simplify deconfliction, the two aircraft are operated at a configurable altitude offset. During Search, the Seeding UA is commanded to track the horizontal position of the Sensing UA while maintaining an altitude offset. This behavior is called Follow, and it ensures that when a suitable location is detected, the Seeding UA is nearby and can quickly begin seeding operations. When seeding is initiated, the Sensing UA transitions to Evaluate and maneuvers to assess the impact of dispersing the seeding material, had it occurred. The evaluation maneuver is modified from the single-aircraft FSM to have the Sensing UA climb away from the seeding point, thus clearing the area for the Seeding UA to begin the seeding maneuver at the flagged seeding location. Once the seeding maneuver has concluded, the Seeding UA is commanded to decrease altitude and return to its last Loiter location. Finally, the Sensing UA is commanded to return to its last Loiter location.

To simplify operations and regulatory compliance, coordination between the two vehicles occurs at the ground station, which issues guidance commands to the aircraft. As continuous, direct communication with each aircraft is required by regulation, this coordination approach does not constitute a significant limitation on the system's capability. This coordination architecture also permits the operator to intervene at any time if required.

Due the the increased scope of the multi-aircraft mission, the single-aircraft state machine must be augmented with two states (Follow, Fly To Seed Point) and one state must be modified. The multi-aircraft FSM is depicted in Figure 15 and summarized in Table 4.

The first additional state is Follow. Follow is only accessible by the Seeding UA, as it commands the aircraft to follow the Sensing UA indefinitely while maintaining the configurable altitude offset. Following behavior is achieved by simply commanding the Seeding UA to the current Sensing UA lateral position. The altitude offset ensures and simplifies deconfliction with the Sensing UA. The Follow state allows the Seeding UA to quickly intercept a seeding location once detected by the Sensing UA. Rapid response is important as the atmospheric features targeted in this campaign persist on the order of minutes (Orlanski, 1975).

The second additional state is Fly To Seed Point. This state is only accessible by the Seeding UA, and is triggered upon flagging of a seeding location by the Sensing UA. In the multi-aircraft mission, the Seeding UA must first travel to the location flagged by the Sensing UA before it enters the Release Seed Material state. This state is the transition between the Follow and Release Seed Material states in the multi-aircraft FSM.

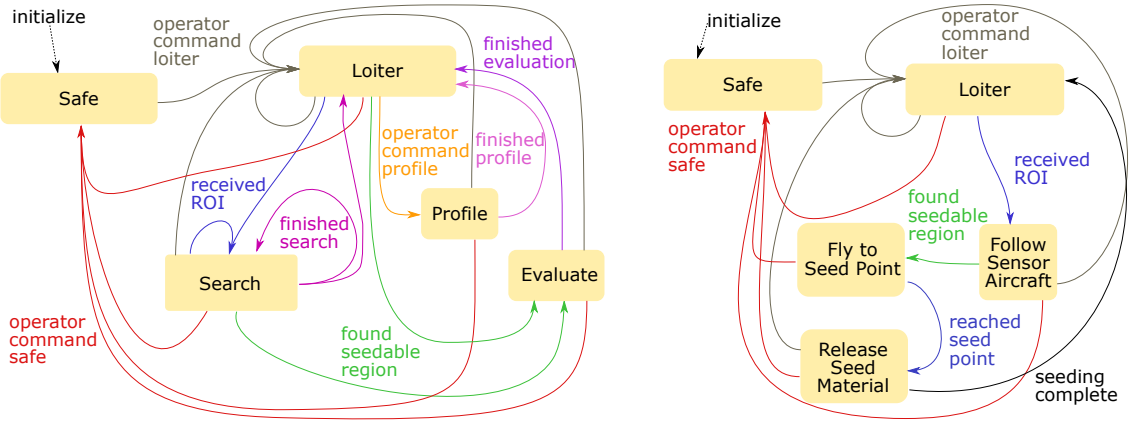

(a) States and transitions which define the behaviors of the Sensing UA.

(b) States and transitions which define the behaviors of the Seeding UA.

Figure 15. The multi-aircraft finite state machine. Division of the machines permits the aircraft to be launched independently, for evaluation to occur simultaneously with seeding, and to continue while the seeding aircraft is recovered.

Table 4. Multi-aircraft mission table of finite state machine states, transitions, and descriptions of states.

State:	Description:	Transitions to:	Transitions from:	Aircraft:
Safe	Inert state, operator must manually activate the autonomy to transition out.	Loiter	Initialization, All states	Sensor, Seed
Loiter	Reposition the aircraft, wait for ROIs to be identified.	Safe, Profile, Search, Seed, Follow	All states	Sensor, Seed
Profile	Take vertical profiles of the atmosphere while orbiting the profile location.	Safe, Loiter	Loiter	Sensor
Search	Fly a search pattern within an ROI, looking for seedable regions.	Safe, Loiter	Loiter, Search	Sensor
Evaluate	Fly an evaluation maneuver relative to the seed point.	Safe, Loiter	Search, Release Seed Material	Sensor
Follow	Perpetually follow the sensing aircraft around, with vertical offset to ensure deconfliction.	Safe, Loiter, Fly to Seed Point	Loiter	Seed
Fly to Seed Point	If not at seed point, fly directly to it to conduct seeding maneuver.	Safe, Loiter, Release Seed Material	Follow	Seed
Release Seed Material	Fly seeding maneuver at seed point and altitude.	Safe, Loiter	Fly to Seed Point	Seed

In the multi-aircraft mission, Evaluate is performed by the Sensing UA contemporaneously with the Seeding UA entering the Fly to Seed Point state. This means modifying one Evaluate input transition to come directly from Search, and be triggered by flagging a seeding location.

4.5. Path Planner

Upon entering the Search state, a path planner immediately generates a search path based on the current target ROI. Search paths are parametrized by a series of waypoints, and are traversed via guidance commands sent from the ground station computer over the MAVLink interface. For this work, the planner assumes an arbitrarily rotated rectangular ROI and is able to generate four types of simple paths: raster (Figure 16), spiral in, spiral out, and diagonal. Raster, spiral in, and diagonal paths are initiated from the closest ROI vertex. Spiral out paths are initiated from the ROI center. Path types are selected by the system operator online based on current conditions and aircraft performance. Paths are specified by waypoints in 3D and are restricted to reside at a constant altitude which can either be specified manually by the operator or automatically by the CSA. Ideally, the search altitude is at cloud base, which is described by the LCL altitude. Other parameters of the path planner include spacing between passes for raster, spiral in, and spiral out paths, and this was set by the operator to be 100 m, the same order of magnitude as the targeted microscale atmospheric features. During operation, raster was the most commonly used pattern, although diagonal paths were also used during periods of rapidly changing atmospheric conditions.

4.6. Human-Robot Interaction and Graphical User Interfaces

A human-robot interface to the autonomy architecture supports an in-field human operator on the loop for both single and multi-aircraft missions, as well as scientific users and mission participants throughout the world. While the uncrewed aircraft system is able to operate fully autonomously without human intervention, the operator is able to interact with various components of the system as a safety measure and in order to initiate specific actions for testing and evaluation. The operator can intervene by manually transitioning the finite state machine between states, changing

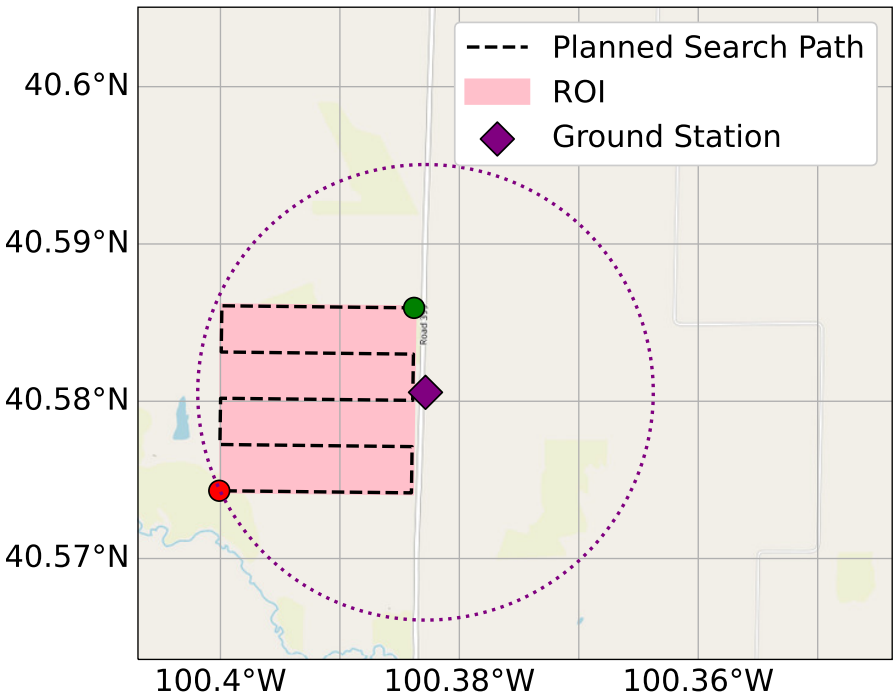

Figure 16. A planned raster search path targeting an ROI received by RECCES during Mission #1 of Flight #9 of the field campaign. Due to FAA restrictions, the ROIs and planned paths were constrained to be within a 1 mile radius of the ground station (dotted purple line) when possible. The search path start and end points are marked with green and red circles, respectively. The aircraft traverses the search path until completion or a seeding location is found.

parameters, and disabling the autonomy altogether. The operator is also able to feed ROIs to the autonomy directly, in case RECCES is unavailable or the in-field meteorologist deems it beneficial to do so. The sUAS operator interacts with a custom GUI interface that is run onboard the ground station computer (Figure 17). This interface provides all relevant information on the system and a control panel to manipulate the system or issue commands. Through this interface, the operator could reliably understand and work with two aircraft during multi-aircraft missions. For the missions described in Section 5, the transition from the Search state to the Seed state was suppressed at the start of the mission until the human operator enabled it. Initiating transition from Safe to Loiter to start the mission and activation of the Search to Seed transition were the main interactions by the operator, otherwise missions were run autonomously.

Members of this project reside around the world, and were not all able to be in the field during deployment. To provide situational awareness and collaboration capabilities with remote members, a web-based *Mission Observation GUI* was developed to display live aircraft telemetry, sensor data, CSA outputs, RECCES ROIs, flight crew locations, and weather radar data. The Mission Observation GUI was accessed by remote members in four different U.S. states, South Africa, and the United Arab Emirates. This interface proved vital for quickly disseminating information regarding current weather and flight conditions, aircraft performance, and autonomy performance.

5. Results

A 3-week-long field campaign was conducted in the U.S. Great Plains during August 2021 to incrementally demonstrate and validate the CONOPS and autonomous system implementation. In this work a "flight" is the time between takeoff and landing for an aircraft. The autonomous

Table 5. Field Deployment Flight Summary.

Flight:	Date:	Time (MT):	Latitude (Deg):	Longitude (Deg):	Aircraft(s):	Flight Time:
1	8/11/2021	3:03 PM	40.145127	−105.241436	SR1	0:46:09
2	8/13/2021	4:28 PM	40.555246	−102.952622	SR1	0:58:28
3	8/18/2021	6:09 PM	40.554651	−103.790896	SR1	1:00:55
4	8/19/2021	1:45 PM	40.002235	−103.036691	SR1	1:22:38
5	8/19/2021	5:28 PM	40.147778	−103.269899	SR1	0:14:19
6	8/25/2021	2:17 PM	40.215696	−101.239072	SR2	0:50:40
7	8/26/2021	6:40 PM	40.801466	−100.950366	SR2	0:42:54
8	8/27/2021	3:01 PM	41.003332	−101.691501	SR2/RAAVEN2	1:37:41
9	8/28/2021	4:48 PM	40.580565	−100.382833	SR1/RAAVEN2	1:19:14

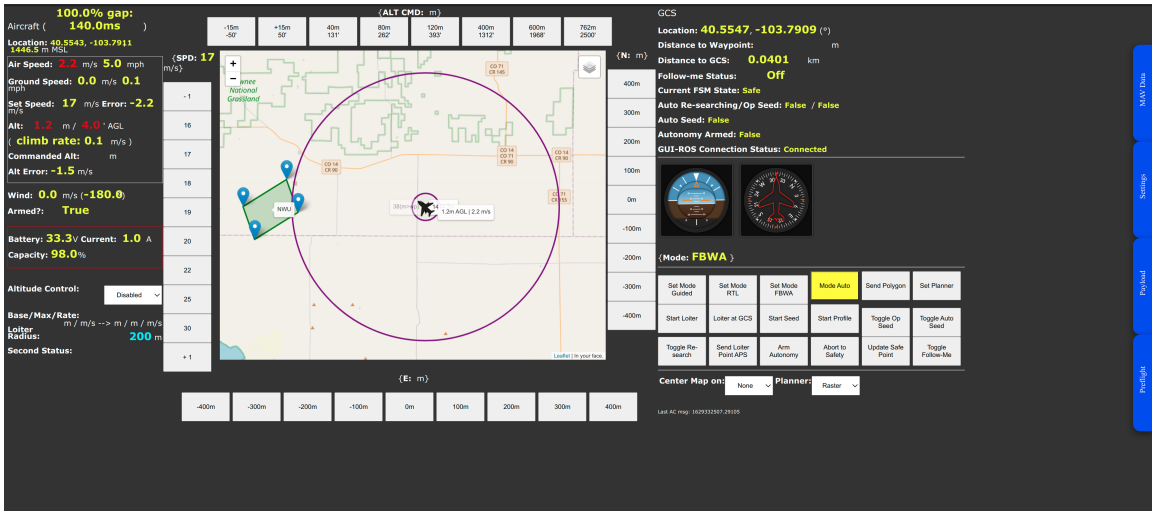

Figure 17. The sUAS operator graphical user interface. This interface provides situational awareness via information regarding current weather conditions, aircraft telemetry, autonomy data, and sensor data. It also allows the operator to manipulate and manually control the autonomy system to improve performance or ensure safety.

concept of operations consists of three phases (Loiter, Search, Seeding) which comprise a single "mission." A mission is completed either by releasing seed material at a seeding location before returning to Loiter or returning to Loiter directly from Search to wait for another ROI (Sections 2 and 4). Therefore, each mission results in at most one seeding event in the single- and multi-aircraft missions. Multiple missions can be conducted during a single flight, and multiple flights can take place on a given day.

The field campaign was structured to incrementally demonstrate components of the overall system. To measure progression and provide milestones to achieve during the field campaign, a series of five Technical Capability Levels (TCLs) were defined (Appendix 8.1). Table 5 summarizes the flights, while Table 6 summarizes the TCL progression during the campaign. Over the course of the 3-week campaign, flights occurred on 9 different days. In total, the system amassed over 8 hours of flight time, approximately 3 hours of which were multi-aircraft flights. Because the campaign was nomadic, two different Sensing UA were deployed, named SR1 and SR2. The first five single-aircraft flights (Flight #1–5) were conducted with SR1 followed by two single-aircraft flights (Flight #6–7) by SR2. The final two flights (Flight #8–9) validated the multi-aircraft CONOPS. The field campaign was scheduled to end on August 28, 2021, thus the decision was made to move to multi-aircraft operations (TCL 3–5) without achieving the stated completion criteria of three

Table 6. Summary of Progression during the Field Campaign.

Flight:	Progression:	Flight Details:
1	——	Aircraft, sensors, and autonomy shakedown flight at testing facility.
2	——	In-field shakedown flight; targeted and successfully intercepted a manual ROI in clear air.
3	——	Received RECCES ROI 10 miles from ground station. Instead, targeted a small nearby storm by manually specifying an ROI with the help of the in-field meteorologist.
4	——	Received RECCES ROI targeting a very fast-moving storm. Attempted to reposition ground station while aircraft was in-flight, but were unable to catch the storm.
5	1x TCL 1 & 2	Autonomously intercepted RECCES ROI and completed a full single-aircraft mission.
6	1x TCL 1 & 2	Autonomously intercepted RECCES ROI, and completed a search which resulted in a seeding maneuver. Had to cut evaluation maneuver short due to reduced visibility with changing weather.
7	——	Received RECCES ROI targeting a fast-moving storm. Ground station was out of position during launch. Attempted to reposition the ground station in-flight, but unable to catch the storm.
8	——	In-field shakedown flight of multi-aircraft and autonomy system in clear air. Successfully completed several missions by manually specifying ROIs and triggering seeding maneuvers.
9	4x TCL 1–5	Completed four full multi-aircraft missions. All missions autonomously targeted RECCES ROIs. No repositioning was necessary, as conditions were favorable at launch site.

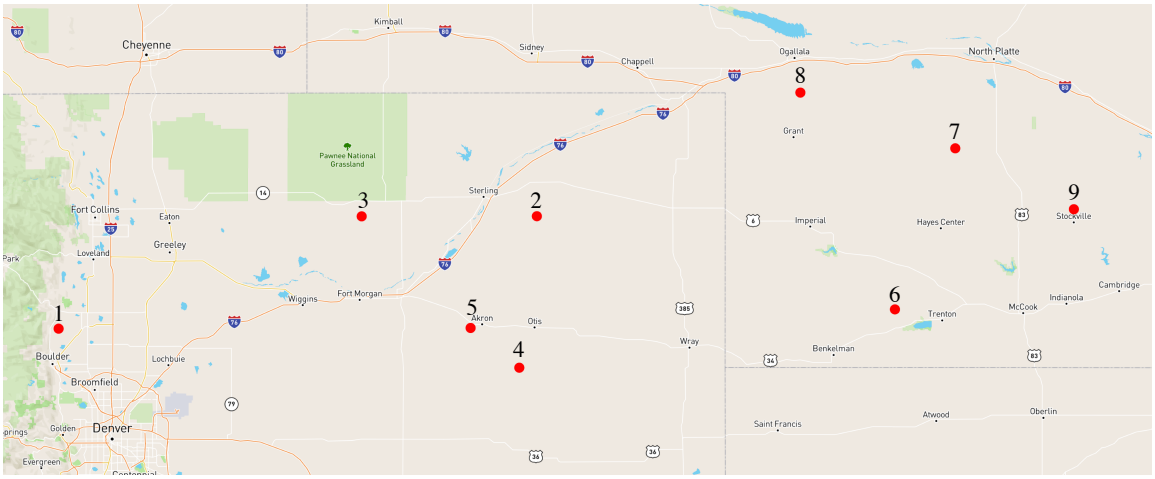

Figure 18. Launch locations of the 9 flights during the August 2021 field campaign.

successful TCL 2 demonstrations. Flight #5 and Flight #9 are good examples of the single-aircraft and multi-aircraft CONOPS, respectively, and are described in more detail in Sections 5.1 and 5.2 below. These two flights were also highly successful in terms of TCL progression, with Flight #9 successfully completing TCLs 1–5 in four successive missions.

A map of all nine flight launch locations is shown in Figure 18. The nomadic CONOPS allowed the field crew to travel hundreds of miles to find suitable conditions in which to conduct the study. Flights #1 and #2 were conducted early in the first week of the field campaign just outside of Boulder, Colorado and in northeast Colorado, respectively. The crew had to wait almost a week for weather conditions to improve for Flights #3–5, which occurred in northeast Colorado around Akron. Almost another week passed before the final group of flights (#6–9) occurred over the last 4 days of the campaign. The final group of flights were the furthest away, all taking place in southwestern Nebraska.

Figure 19. The Super RAAVEN ready to launch the evening of August 19th to start Flight #5 of the campaign. An encroaching storm can be seen in the background.

5.1. Flight #5: August 19 2021

On the morning of August 19, 2021 the meteorological team forecasted there would be significant convection forming just east of Fort Morgan, CO in the early afternoon. This was informed by forecasts from the ECMWF and HRRR weather models, as well as soundings from the North Platte, NE weather station. For Flight #4, the team deployed SR1 as the Sensing UA to intercept a storm system developing southeast of Akron, CO at approximately 1:45 pm MT. Flight #4 was too late to catch the targeted cell. The crew attempted to reposition while the aircraft was in flight using a mobile tracking behavior (Frew et al., 2020a), but the storm dissipated too quickly to be intercepted.

A second opportunity arose late afternoon of August 19, when a suitable storm system (Figure 19) was identified to the west of Akron, CO. Figure 20a shows the radar reflectivity of the storm when the team chose the flight area, indicated by the light blue circle in front of the path of several encroaching storm cells. The team launched the SR1 for a single-aircraft flight at approximately 5:28 pm MT. At launch, the RECCES algorithm identified an ROI directly above the aircraft, and the sUAS autonomy was initialized in Safe (Figure 21a). The operator immediately commanded the aircraft to ascend to the 2500 ft (762 m) AGL flight ceiling, while activating the autonomy by transitioning to Loiter (Figure 21b). After just half an orbit, the system was transitioned to Search, as the aircraft was within a candidate storm cell. The aircraft flew a search pattern within the ROI (Figure 21c). After one leg of the search pattern was completed, the CSA identified a seeding location within the ROI, the aircraft automatically transitioned to the Release Seed Material state, and flew a seeding maneuver (Figure 21d). Following the completion of the seeding maneuver, an Evaluation maneuver was flown (Figure 21e). After the evaluation behavior was completed, the system returned to Loiter (Figure 21f), completing the mission. At this point, the aircraft and crew were being lightly rained on, with heavy rain and wind imminent. Figure 20b shows the radar reflectivity and ground station at the time the aircraft landed. The decision was made to manually pilot the aircraft and land as soon as possible. The aircraft was safely landed before severe weather (the dark red and pink in the radar reflectivity image) arrived.

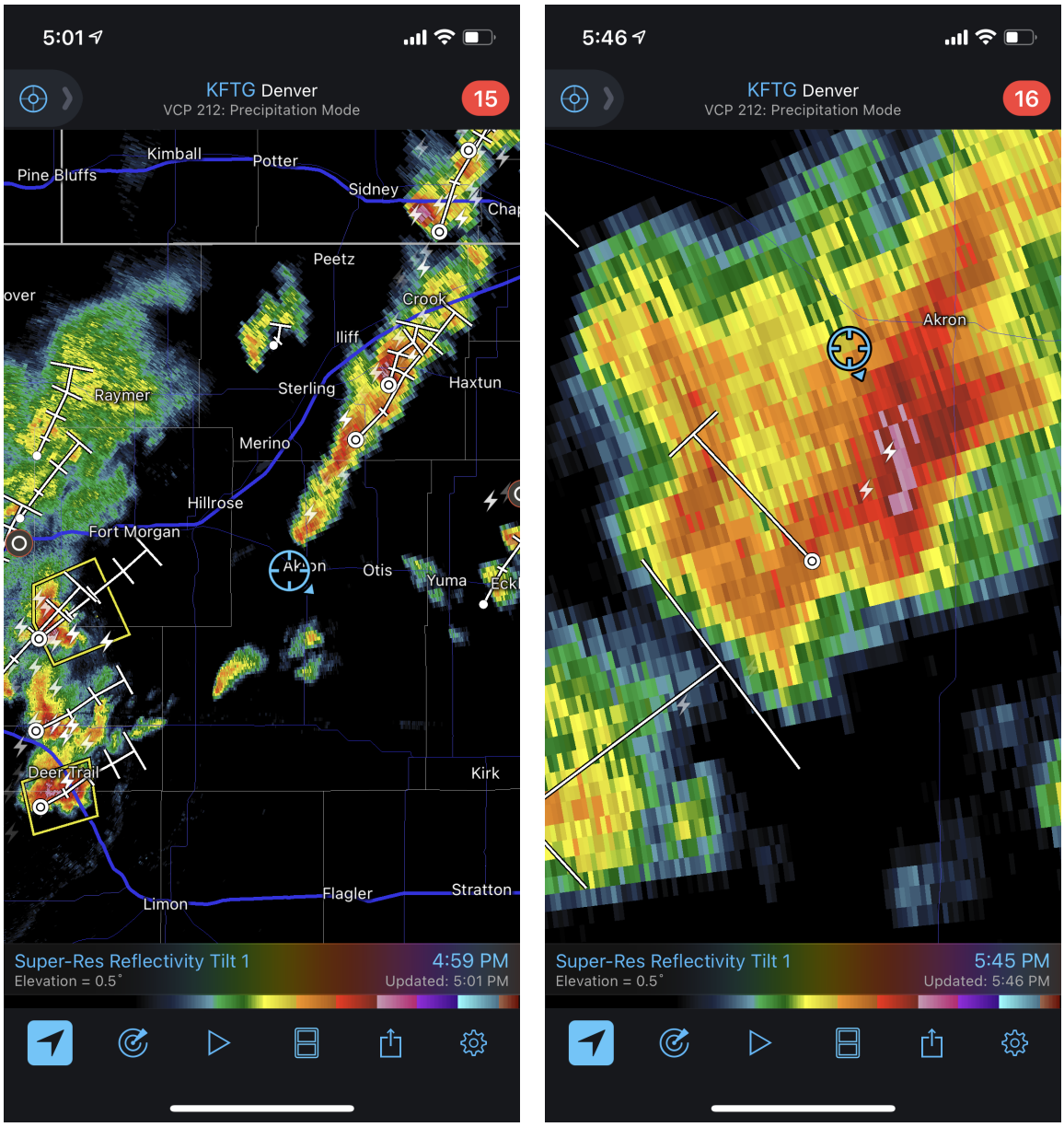

Figure 20. Radar reflectivity images from Flight #5 a.) when the flight operations area was chosen and b.) when the aircraft landed. These images use the standard reflectivity color scale of the National Weather Service where the scale shows the strength of returned energy to the radar which is correlated to the intensity of the precipitation. The light blue circle indicates the location of the flight crew and ground station.

This flight consisted of the first complete mission that took place fully within an ROI. Furthermore, the system was able to identify and act upon a seeding location within the ROI. This mission satisfied TCL 1 & 2, and was the first successful TCL demonstration of the field deployment. The operator interface gave the operator full situational awareness of the FSM, RECCES, and encroaching weather (via NEXRAD data streams), enabling the human-robot team to make quick decisions for mission success. It should be noted this flight had some hardware reliability issues. Before launch, the crew noticed a broken GPS cable, which prevented the MIP sensor from finding a localization solution. This was swapped in a matter of minutes. A second repair was necessary

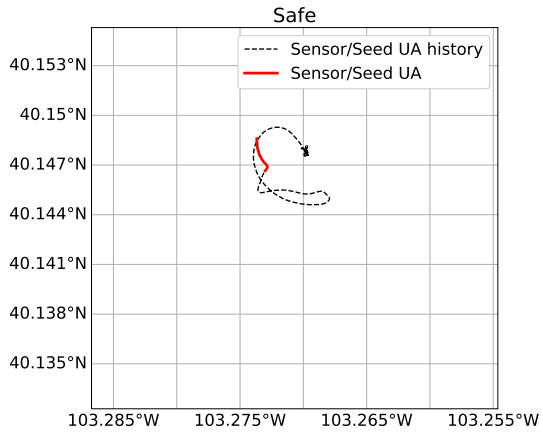

(a) Having been launched, aircraft is initialized in the Safe state.

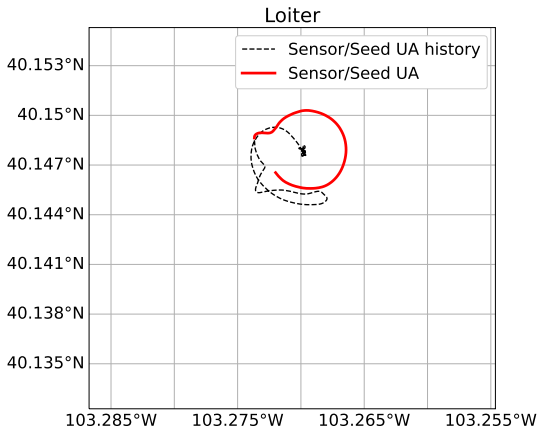

(b) Operator activates the autonomy system and transitions to Loiter.

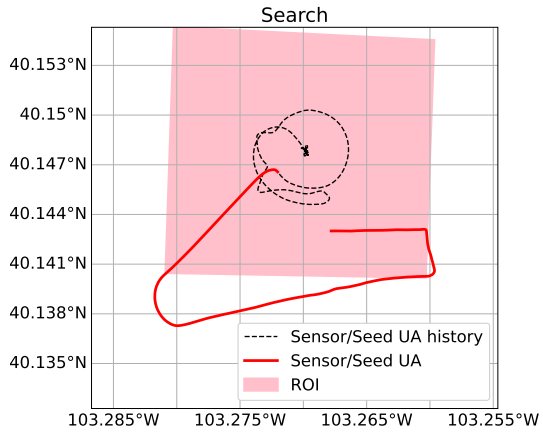

(c) An ROI is determined and the system is commanded to begin searching.

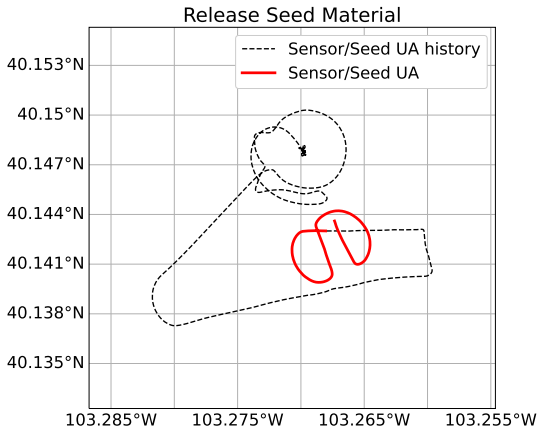

(d) A seeding location is detected, and triggers a transition to Release Seed Material.

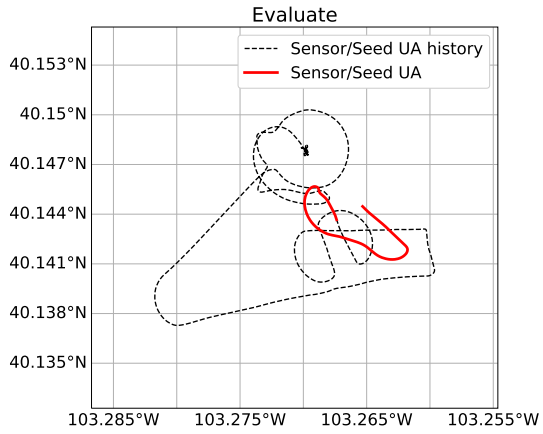

(e) An evaluation maneuver is immediately conducted after seeding to record changes in atmospheric state.

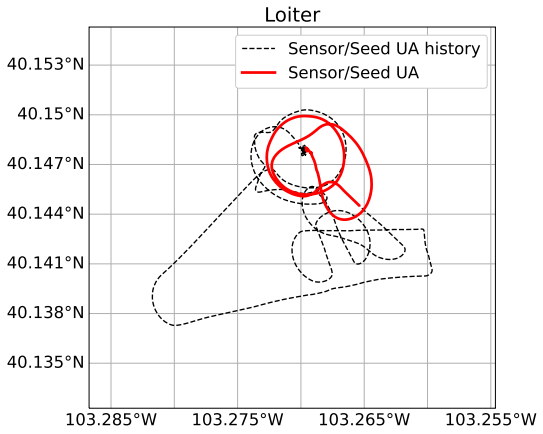

(f) The system returns to Loiter to await further instructions.

Figure 21. The single aircraft mission completed during Flight #5 on August 19, 2021. Plot titles indicate the state of the system.

Figure 22. The Super RAAVEN taking off the evening of August 28 2021 to intercept a storm system during Flight #9 of the campaign. The RAAVEN launched shortly after, initializing the coordinated multi-aircraft flight.

to fix the CDP, which was not responding to data request commands from the BeagleBone Green companion computer. The crew swapped this sensor out in the field as well, though this repair took much longer.

5.2. Flight #9: August 28, 2021

The morning of August 28, 2021, the meteorological team forecasted that storm systems would likely form over Nebraska, forced by an impending cold front. All of the numerical weather forecasting models showed strong agreement that convection would occur along the front. The team concurred that a deployment around Lexington, NE was likely, though the deployment location (Figure 22) would be determined closer to the launch time.

At 4:10 pm MT, a launch site was identified just north of Stockville, NE. At 4:52 pm MT, SR1 (Sensing UA) was launched to intercept an impending storm cell. The team launched the RAAVEN (Seeding UA) just a few minutes after. Both aircraft were initialized to Safe (Figure 23a), and the Sensing UA was commanded to the altitude ceiling of 2500 ft (762 m) AGL. The Seeding UA simultaneously ascended to maintain the commanded altitude offset. At this point, the crew and both aircraft were within an ROI identified by RECCES. The autonomy for both aircraft was activated by the operator, transitioning momentarily to Loiter (Figure 23b). The Seeding UA was commanded into Follow by the operator while the Sensing UA transitioned to Search, driven by an updated ROI (Figure 23c). After completing two legs of a raster search path (Figure 16), the Sensing UA identified a seeding location, at which point it transitioned to Evaluate while the Seeding UA transitioned to Fly To Seed Point, and then to Release Seed Material (Figure 23d). This concluded the first mission of Flight #9, and was the first successful multi-aircraft mission within an ROI. This mission successfully demonstrated TCL 1-5, the first mission to do so.

Over the course of the 1 hour and 19 minute flight, the sUAS completed a total of four complete missions, all of which were inside of an ROI identified by RECCES. Each of these missions successfully demonstrated TCL 1–5. Figure 24 shows radar reflectivity images from two moments

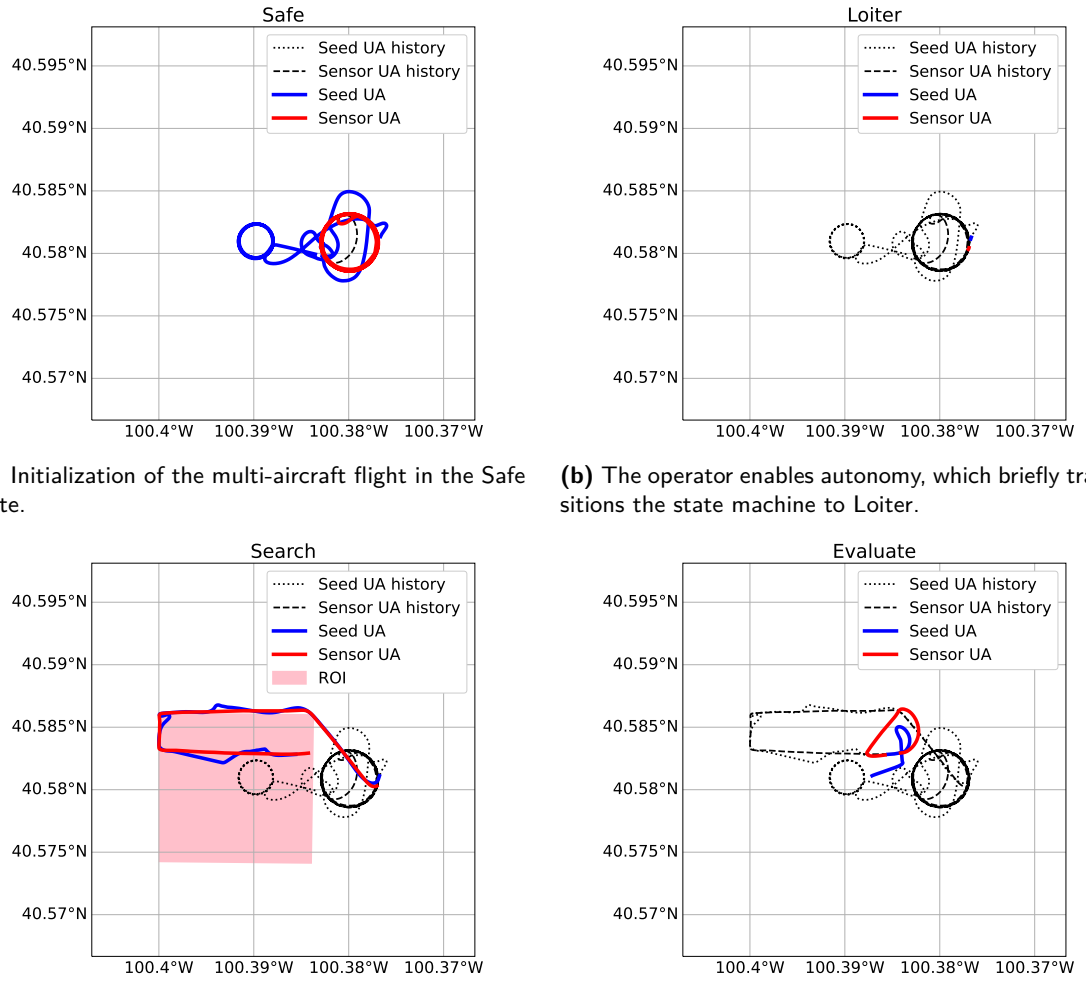

(a) Initialization of the multi-aircraft flight in the Safe state.

(b) The operator enables autonomy, which briefly transitions the state machine to Loiter.

(c) The system receives ROI, so the FSM is transitioned to Search. The sensor aircraft begins flying a search, while the seed aircraft follows.

(d) The sensing aircraft finds a seeding location within the ROI, as indicated by the CSA score. Seeding and evaluation maneuvers commence.

Figure 23. Mission #1 completed during Flight #9 on August 28, 2021. Plot titles indicate the state of the Sensor UA.

during the flight. The aircraft were successfully coordinated primarily by the autonomy system, with some high-level decisions made by the operator. During this flight, the primary decisions made by the operator were enabling the autonomy and manually repositioning the aircraft team between missions with the help of the in-field meteorologist. See Figure 23 for the complete flight tracks of mission #1 completed during this flight. See the Appendix (Section 8) for missions #2–4 from this flight (Figures 28–30).

Figure 25 shows flight tracks overlayed with the seed score and locations of the five seeding events. This figure demonstrates the CSA's ability to make decisions distinguishing seedable from unseedable regions of the atmosphere in real time. Conditions during this flight were very good for seeding, therefore any location with a strong vertical wind speed had a high seed score. Locations with low or negative vertical wind speed had near-zero seed scores, due to the inherent ineffectiveness of deploying seeding material in these locations. The result is a near-binary seed score.

Flight #9 demonstrated the effectiveness of human-robot teaming to complete a complex task with multiple aircraft. The autonomy handled lower level tasking and coordination, allowing the

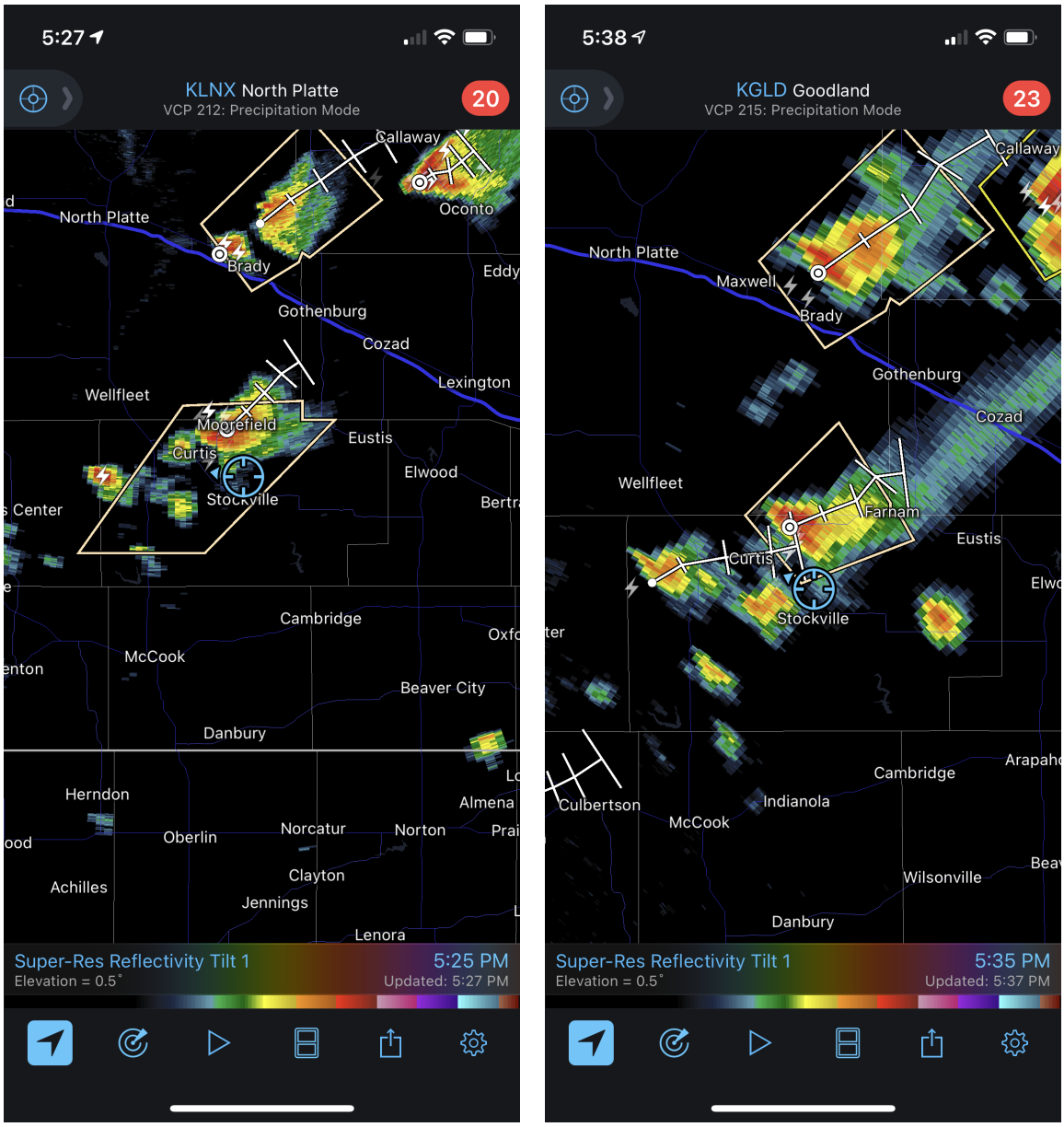

Figure 24. Radar reflectivity images from Mission 2 during Flight #9 a.) when both aircraft are in Safe modes waiting to begin the mission and b.) when the mission was completed. These images use the standard reflectivity color scale of the National Weather Service where the scale shows the strength of returned energy to the radar which is correlated to the intensity of the precipitation. The light blue circle indicates the location of the flight crew and ground station. The light yellow polygons are thunderstorm watches issued by the National Weather Service.

operator to focus on high-level decision making and situational awareness. The Seeding UA took an average of 10 seconds to travel to the identified seeding locations in Flight #9, demonstrating the viability of the system to target micro scale atmospheric features which exist on the order of minutes. The distributed autonomy architecture enabled data to be intelligently processed and shared across nodes in the computation graph. Finally, the CSA algorithm was able to guide behaviors of both the sensor and seed aircraft. Flight #9 was the successful culmination of the flight campaign designed to incrementally validate the complete autonomous small uncrewed aircraft system.

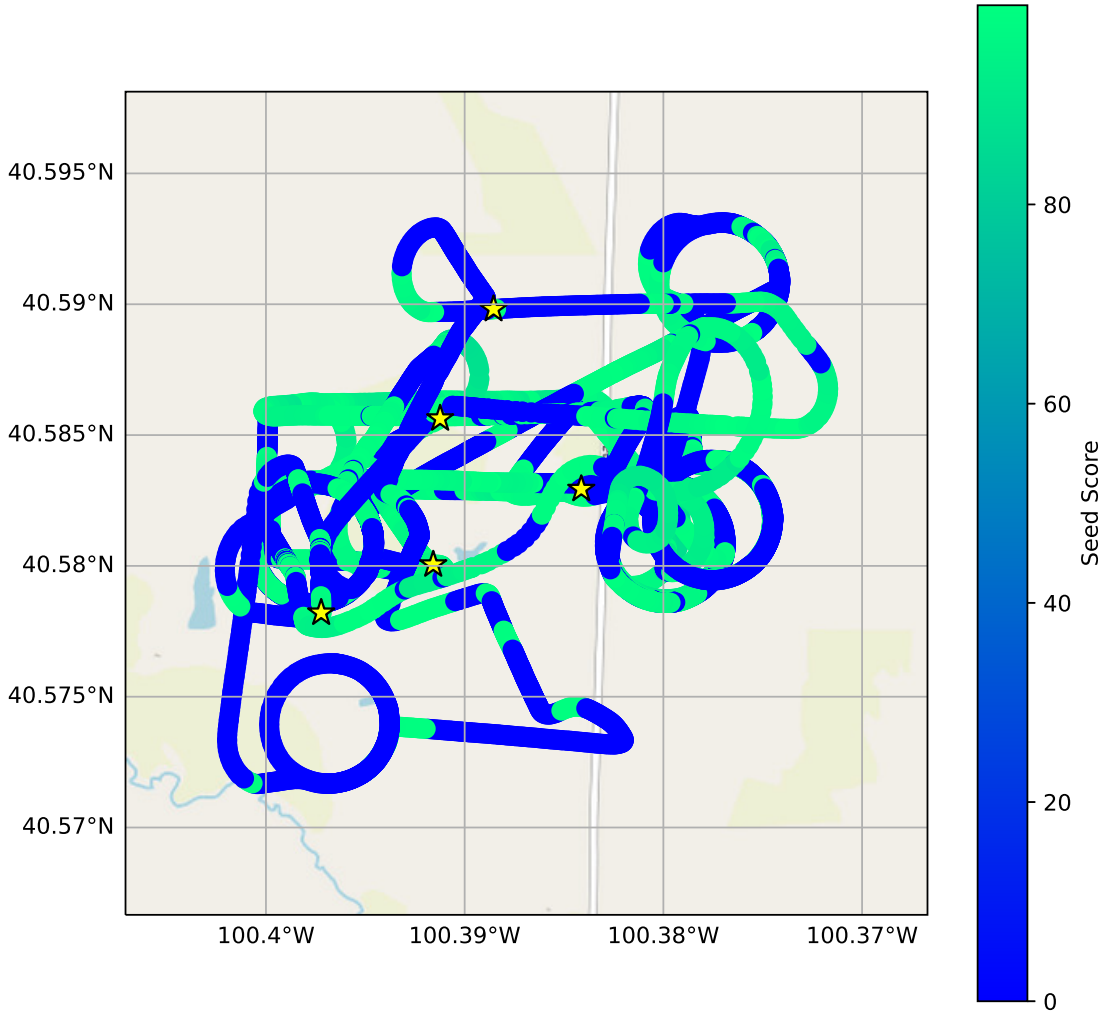

Figure 25. Flight tracks from Flight #9 on August 28, 2021, with seed score overlayed. Stars indicate locations where seeding maneuvers were initiated.

6. Discussion

The successful deployment of the targeted observation sUAS can be attributed to three key factors. First, the autonomy (RECCES, CSA, FSM) and various support systems (remote servers, Mission Observation GUI) allowed for a clean, concise, and informative set of information to be communicated to the operator and other project members. By only passing relevant, mission-critical information to the operator, the autonomy allowed the operator to focus on mission-level problems. This is especially important during storm sampling missions in areas such as the U.S. Great Plains, where features develop and move quickly, requiring fast operator decision-making. Furthermore, it freed up enough operator attention to simultaneously operate two aircraft in a complex coordinated mission (Figure 26). The second key to success was the ruggedized and custom-built aircraft, avionics, and scientific sensor suite, which allowed for reliable sUAS operations in the field. Two of the three onboard sensors (MIP, CDP) were specialized for sUAS application, meaning they were smaller and lighter than their crewed aircraft equivalents. The POPS was not designed to be flown on an sUAS, but performed reliably. As targeted observations of the atmosphere using sUAS become more common, it will be critical for sensor manufacturers to produce lighter and smaller units, as this has a direct and significant impact on sUAS performance. The final key to success was

Figure 26. The view from the following Seeding UA of the Sensing UA during a two-aircraft mission.

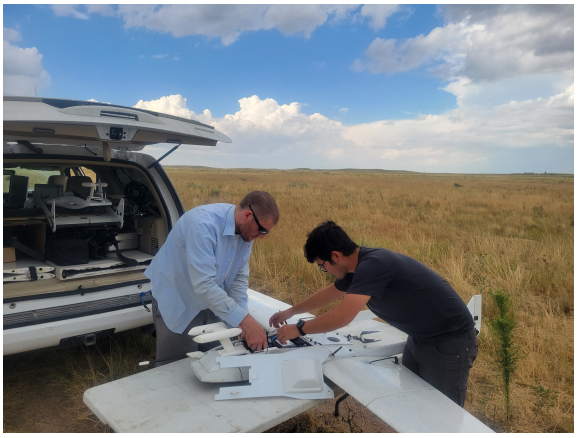

Figure 27. A knowledgeable and experienced flight crew made reliably flying a complex sUAS feasible during the field campaign.

the professional, highly experienced flight crew, who have been conducting severe storm research with sUAS for over a decade (Figure 27). The crew enabled effective aircraft operations, hardware troubleshooting, airspace reconnaissance, and decision-making regarding all other aspects of daily field campaign operations.

Despite the overall success of the field deployment, there are several opportunities for improvement for future multi-aircraft targeted atmospheric observation sUAS missions. First is the centralized architecture of the autonomy system. All communications and decisions were routed through the primary ground station computer. While this architecture allowed for fast development and isolated troubleshooting, it makes reliable cellular communications and ground station computer operations mission critical. Ideally, a networking and computing architecture with multiple fail-safes for component failures would enable more robustness to various anomalies encountered during an extended field campaign such as this. Second, future work should explore the formulation and quantification of prior beliefs of seedable regions occurring over the operational domain. This could potentially be done using climatology data, satellite imagery, or even onboard vision data. A prior belief would help inform more efficient planning procedures, such as ergodic planning (Miller and Murphey, 2013), reducing search times and enabling the system to conduct more missions during a single flight. Another opportunity for future work is enhancing the scalability of deployable

robotic teams while retaining a single human operator. Though this work demonstrated a successful deployment with two aircraft, the present system would not scale to tens or hundreds of aircraft. Finally, previous deployments of the RAAVEN aircraft (Frew et al., 2020a) demonstrated the importance of fast deployment for storm interception in the Great Plains region. Due to the size and weight of the Super RAAVEN, the flight crew was unable to use the rapid launch system developed for TORUS 2019. Instead, the crew utilized a bungee system to launch the aircraft. While this was simple and effective, it took upwards of 30 minutes to prepare and launch the aircraft. This placed a heavy reliance on the now-casting abilities of the in-field meteorologists to determine launch sites which intersected a suitable storm track.

7. Conclusion

This paper presents results from a 3-week-long field deployment of a small uncrewed aircraft system for targeted observation of preconvective storm cells in the U.S. Great Plains. A concept of operations of the cloud seeding mission is presented, including regulation requirements that motivated some design choices of the system. The problem of studying preconvective cells is detailed, and motivated the need for targeted in situ sensing of relevant microscale atmospheric features. The Super RAAVEN aircraft, along with sensing, computing, and avionics components, proved to be reliable and allowed for consistent deployments when weather was favorable. We leveraged a dispersed autonomy architecture to enable complex algorithms to be integrated with limited fielded computational resources. The autonomy modules were presented, and consist of the storm tracking algorithm RECCES, cloud seeding algorithm, and the finite state machine. The utility of efficiently incorporating a human operator on-the-loop was demonstrated, as it allows the operator to conduct decision making and continuously interface with scientific experts from around the world. Finally, we presented the results from two particularly successful single and coordinated multi-aircraft flights which highlighted the significant progression achieved over the course of the campaign, as measured by Technical Capability Levels (Section 8).

Small uncrewed aircraft systems provide a versatile, economic, and reliable means for remote and in situ sensing of important natural phenomena. This study demonstrates one application, namely targeted observations for sensing and quantifying microscale atmospheric features with applications to cloud seeding. Via the system and software developments presented, this work is a significant step towards precision cloud seeding operations with autonomous sUAS, and it is the first fielded demonstration of such technology.

Acknowledgments

This work was supported by the United Arab Emirates Rain Enhancement Program. Thanks to the University of Colorado Boulder Integrated Remote and In Situ Sensing (IRISS) program for hardware and flight support. Additional thanks to the field deployment flight crew, whose members included Steve Borenstein, Chris Choate, Michael Rhodes, Ceu Gomez-Faulk, and Dan Breed.

ORCID

C. Alexander Hirst https://orcid.org/0000-0001-8841-1231
John Bird https://orcid.org/0009-0000-7967-3766
Roelof Burger https://orcid.org/0000-0002-4359-4588
Henno Havenga https://orcid.org/0000-0002-9238-0295
Gerhardt Botha https://orcid.org/0000-0003-3194-9449
Darrel Baumgardner https://orcid.org/0000-0002-3296-3085
Tom DeFelice https://orcid.org/0000-0002-2282-4890
Duncan Axisa https://orcid.org/0000-0002-7406-9049
Eric Frew https://orcid.org/0000-0003-3686-089X

References

Andreae, M., and Rosenfeld, D. (2008). Aerosol–cloud–precipitation interactions. part 1. the nature and sources of cloud-active aerosols. *Earth-Science Reviews*, 89(1-2):13–41.

ArduPilot (2019). Open Source Drone Software. Versatile, Trusted, Open. Ardupilot. http://www.ardupilot.org/.

Axisa, D., and DeFelice, T. P. (2016). Modern and prospective technologies for weather modification activities: A look at integrating unmanned aircraft systems. *Atmospheric Research*, (178-179):114–124.

Bird, J. J., Langelaan, J. W., Montella, C., Spletzer, J., and Grenestedt, J. L. (2014). Closing the loop in dynamic soaring. In *AIAA Guidance, Navigation, and Control Conference*, page 0263.

Davis, K. D. (2008). Interim Operational Approval Guidance 08-01 - Unmanned Aircraft Systems Operations in the US National Airspace System. *Interim Operational Approval Guidance*, AIR-160.

de Boer, G., Borenstein, S., Calmer, R., Cox, C., Rhodes, M., Choate, C., Hamilton, J., Osborn, J., Lawrence, D., Argrow, B., et al. (2021). Measurements from the university of colorado raaven uncrewed aircraft system during atomic. *Earth System Science Data Discussions*, pages 1–22.

DeFelice, T., and Axisa, D. (2016). Developing the Framework for Integrating Autonomous Unmanned Aircraft Systems into Cloud Seeding Activities. *Journal of Aeronautics & Aerospace Engineering*, 5(3).

DeFelice, T., and Axisa, D. (2017). Modern and prospective technologies for weather modification activities: Developing a framework for integrating autonomous unmanned aircraft systems. *Atmospheric Research*, 193:173–183.

Depenbusch, N. T., Bird, J. J., and Langelaan, J. W. (2018a). The AutoSOAR autonomous soaring aircraft, part 1: Autonomy algorithms. *Journal of Field Robotics*, 35(6):868–889.

Depenbusch, N. T., Bird, J. J., and Langelaan, J. W. (2018b). The AutoSOAR autonomous soaring aircraft part 2: Hardware implementation and flight results. *Journal of Field Robotics*, 35(4):435–458.

Dixon, M., and Seed, A. (2014). Developments in echo tracking - enhancing titan. In *ERAD 2014 - The eighth European conference on radar in meteorology and hydrology developments*, pages 1–14. ERAD.

Dixon, M., and Wiener, G. (1993). TITAN: thunderstorm identification, tracking, analysis, and nowcasting - a radar-based methodology. *Journal of Atmospheric & Oceanic Technology*, 10(6):785–797.

Elston, J., Stachura, M., Argrow, B., Frew, E., and Dixon, C. (2011a). Guidelines and best practices for faa certificate of authorization applications for small unmanned aircraft. In *AIAA Infotech@Aerospace*, St. Louis, MO. AIAA.

Elston, J. S., Roadman, J., Stachura, M., Argrow, B., Houston, A., and Frew, E. W. (2011b). The tempest unmanned aircraft system for in situ observations of tornadic supercells: Design and vortex2 flight results. *Journal of Field Robotics*, 28(4):461–483.

Frew, E., Argrow, B., Borenstein, S., Swenson, S., Hirst, A., Havenga, H., and Houston, A. (2020a). Field observation of tornadic supercells by multiple autonomous fixed-wing drones. *Journal of Field Robotics*, 37(6):1077–1093.

Frew, E., Glasheen, K., Hirst, A., Bird, J., and Argrow, B. (2020b). A dispersed autonomy architecture for information-gathering drone swarms. In *IEEE Aerospace Conference*, Big Sky, MT.

Hattenberger, G., Verdu, T., Maury, N., Narvor, P., Couvreux, F., Bronz, M., Lacroix, S., Cayez, G., and Roberts, G. C. (2022). Field report: deployment of a fleet of drones for cloud exploration. *International Journal of Micro Air Vehicles*, 14:17568293211070830.

Heistermann, M., Collis, S., Dixon, M., Giangrande, S., Helmus, J., Kelley, B., Koistinen, J., Michelson, D., and Peura, M. (2015). The emergence of open-source software for the weather radar community. *Bulletin of the American Meteorological Society*, 96(1):117–128.

Howell, W. E. (1949). The growth of cloud drops in uniformly cooled air. *Journal of the Atmospheric Sciences*, 6(2):134–149.

Jensen, A. A., Pinto, J. O., Bailey, S. C., Sobash, R. A., de Boer, G., Houston, A. L., Chilson, P. B., Bell, T., Romine, G., Smith, S. W., et al. (2021). Assimilation of a coordinated fleet of uncrewed aircraft system observations in complex terrain: Enkf system design and preliminary assessment. *Monthly Weather Review*, 149(5):1459–1480.

Keating, F., Mitchell, T., Kidd, J., and Jacob, J. D. (2016). Wildfire plume tracking and dynamics using uas. In *AIAA Infotech@ Aerospace*, page 1005.

Miller, L. M., and Murphey, T. D. (2013). Trajectory optimization for continuous ergodic exploration. In *2013 American Control Conference*, pages 4196–4201. IEEE.

NOAA (2015). NEXRAD on AWS. https://registry.opendata.aws/noaa-nexrad/.

NOAA (2017). NOAA Geostationary Operational Environmental Satellites (GOES) 16 & 17. https://registry.opendata.aws/noaa-goes/.

Orikasa, N., Murakami, M., Tajiri, T., Zaizen, Y., and Shinoda, T. (2020). In Situ Measurements of Cloud and Aerosol Microphysical Properties in Summertime Convective Clouds over Eastern United Arab Emirates. *SOLA*, 16(0).

Orlanski, I. (1975). A rational subdivision of scales for atmospheric processes. *Bulletin of the American Meteorological Society*, pages 527–530.

Prevot, T., Rios, J., Kopardekar, P., Robinson III, J. E., Johnson, M., and Jung, J. (2016). UAS Traffic Management (UTM) Concept of Operations to Safely Enable Low Altitude Flight Operations. In *16th AIAA Aviation Technology, Integration, and Operations Conference*.

Quigley, M., Conley, K., Gerkey, B., Faust, J., Foote, T., Leibs, J., Wheeler, R., Ng, A. Y., et al. (2009). Ros: an open-source robot operating system. In *ICRA workshop on open source software*, volume 3, page 5. Kobe, Japan.

Roseman, C. A., and Argrow, B. M. (2020). Weather hazard risk quantification for sUAS safety risk management. *Journal of Atmospheric and Oceanic Technology*, 37(7):1251–1268.

Rosenfeld, D., Axisa, D., Woodley, W. L., and Lahav, R. (2010). A quest for effective hygroscopic cloud seeding. *Journal of Applied Meteorology and Climatology*, 49(7):1548–1562.

Silva, W., and Frew, E. W. (2016). Experimental assessment of online dynamic soaring optimization for small unmanned aircraft. In *AIAA SciTech Forum*, San Diego, CA.

Tang, L., and Shao, G. (2015). Drone remote sensing for forestry research and practices. *Journal of Forestry Research*, 26(4):791–797.

Verdu, T., Maury, N., Narvor, P., Seguin, F., Roberts, G., Couvreux, F., Cayez, G., Bronz, M., Hattenberger, G., and Lacroix, S. (2020). Experimental flights of adaptive patterns for clouds exploration with uavs. In *International Symposium on Experimental Robotics*, pages 17–27. Springer.

Whitley, P. (2020). Unmanned Aircraft Systems Traffic Management Concept of Operations 2.0. Technical report.

How to cite this article: Hirst, C. A., Bird, J., Burger, R., Havenga, H., Botha, G., Baumgardner, D., DeFelice, T., Axisa, D., & Frew, E. (2023). An autonomous uncrewed aircraft system performing targeted atmospheric observation for cloud seeding operations. *Field Robotics, 3*, 687–724.

8. Appendix

8.1. Technical Capability Level Demonstrations

The field campaign was structured as a series of increasingly complex Technical Capability Level (TCL) demonstrations. These TCL demonstrations were designed to show a subset of the capabilities of the UAS, with progressive TCL built on the prior demonstration. This structured approach allowed the flight team to verify subsystem components before adding additional components to the system. Because the field campaign was of limited duration, a small number of successful demonstrations was required before moving on to the next TCL. Further, all system components were running for most of the flights, so multiple TCL could be demonstrated with one flight. The TCL approach defined levels of success, not an order in which components had to be brought online in the autonomy architecture.

TCL 1. *Description*: Sensing UA directed by RECCES to region of interest (ROI), conducts search behavior.

Success criteria: UAS receives accurate ROI and searches it.

TCL completion: TCL 1 will successfully complete at least 1 flight before moving to TCL 2.

TCL 2. *Description*: Sensing UA directed by RECCES to ROI, conducts search behavior, uses CSA to determine the seeding location (SL).

Success criteria: UAS receives accurate ROI, searches it, reports results of CSA over entire ROI, and identifies an SL if CSA determines appropriate conditions.

TCL completion: TCL 2 will successfully complete at least 3 flights before moving to TCL 3.

TCL 3. *Description*: Sensing UA conducts operation in TCL 2, Seeding UA flown at the same time in same area of operations.

Success criteria: Seeding UA flies for over 30 minutes while Sensing UA simultaneously conducts its mission.

TCL completion: TCL 3 will successfully complete at least 2 flights before moving to TCL 4.

TCL 4. *Description*: Sensing UA directed by RECCES to ROI, conducts search behavior, uses CSA to determine an SL, Seeding UA autonomously commanded to the SL, Seeding UA conducts virtual seeding (command autonomously issued but no material dispersed).

Success criteria: Seeding UA receives an accurate SL from Sensing UA and searches it. Sensing UA flies near Seeding UA and reports results of CSA near the SL, and identifies SL if CSA determines appropriate conditions.

TCL completion: TCL 4 will successfully complete at least 3 flights before moving to TCL 5.

TCL 5. *Description*: Sensing UA and Seeding UA conduct operations in TCL 4, Sensing UA conducts seeding assessment maneuvers.

Success criteria: Seeding UA receives an accurate SL from Sensing UA. Sensing UA flies near Seeding UA and reports results of CSA near the SL, and identifies an SL if CSA determines appropriate conditions. Sensing UA issues seeding command to Seeding UA and then performs assessment maneuver.

TCL completion: TCL 5 will successfully complete at least 2 flights before field campaign ends.

8.2. Flight #9 Additional Mission Plots

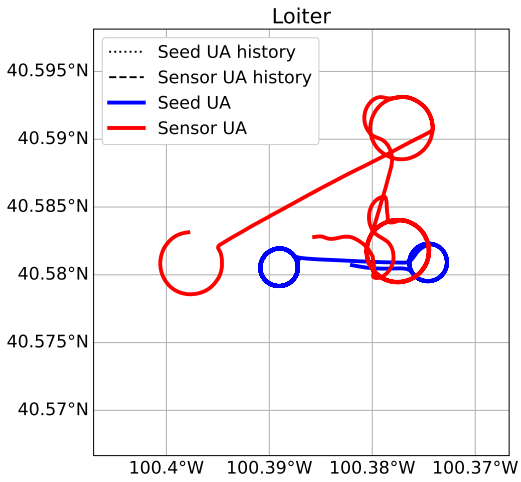

(a) After completing mission #1, both aircraft return to Loiter.

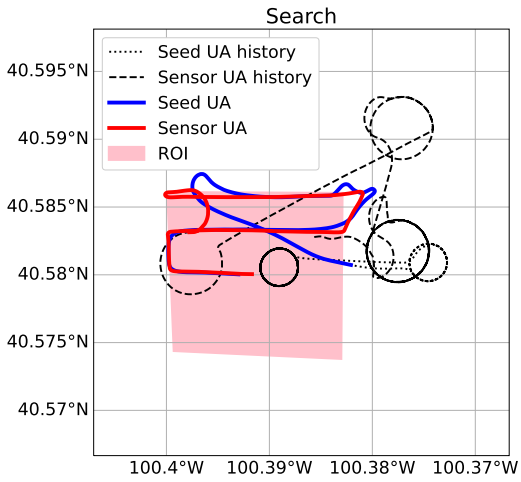

(b) Another ROI is identified by RECCES and the operator. A coordinated search begins.

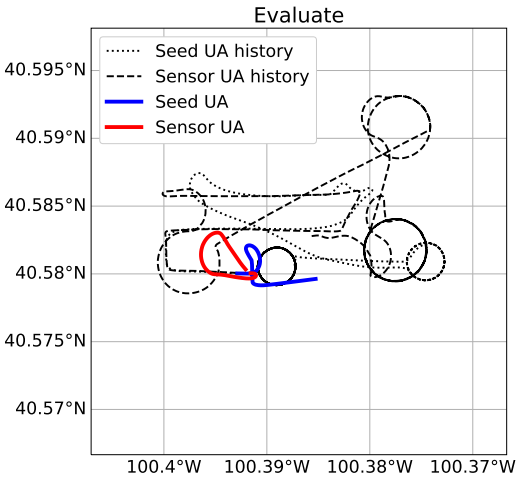

(c) A seeding location is identified, and a seeding maneuver is performed and the mission is completed.

Figure 28. Mission #2 completed during Flight #9 on August 28, 2021. Plot titles indicate the state of the Sensor UA.

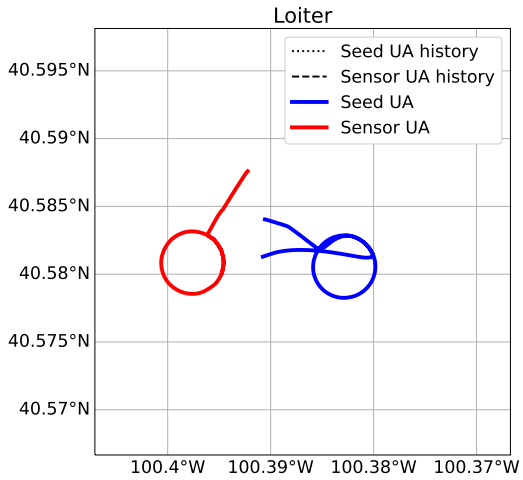

(a) After completing mission #2, both aircraft return to Loiter.

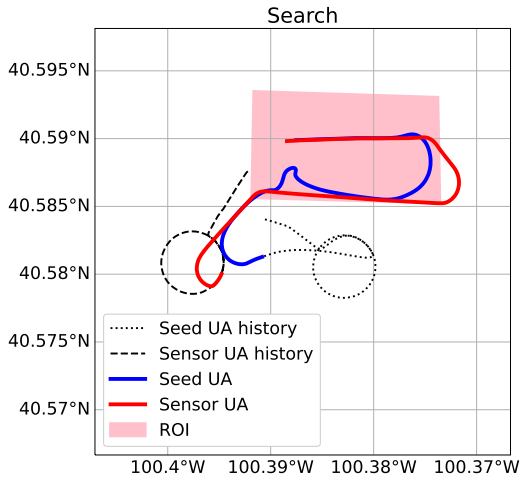

(b) Another ROI is identified by RECCES and the operator. A coordinated search begins.

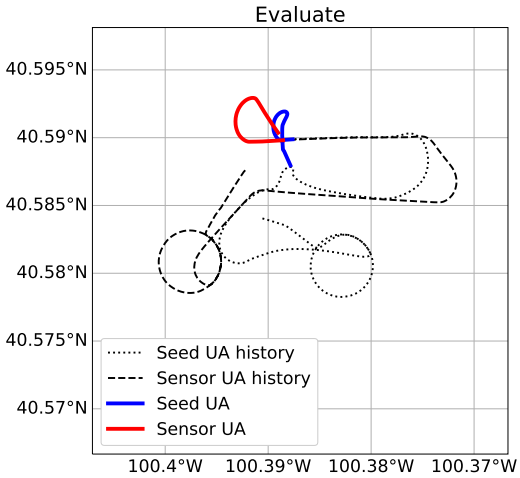

(c) A seeding location is identified, and a seeding maneuver is performed, completing mission #3.

Figure 29. Mission #3 completed during Flight #9 on August 28, 2021. Plot titles indicate the state of the Sensor UA.

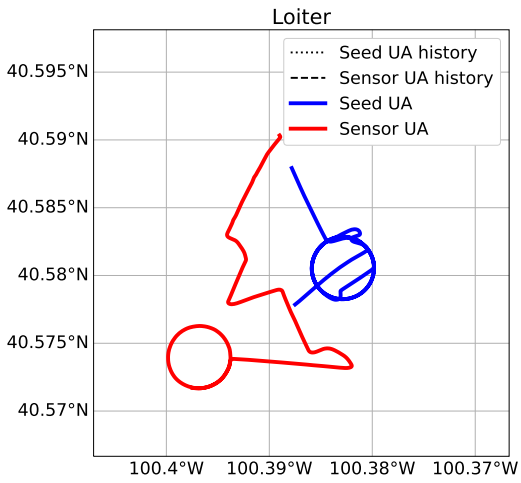

(a) After completing mission #3, both aircraft return to Loiter.

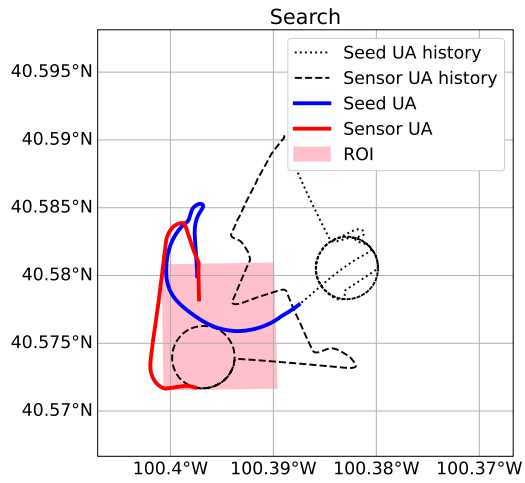

(b) Another ROI is identified by RECCES and the operator. A coordinated search begins.

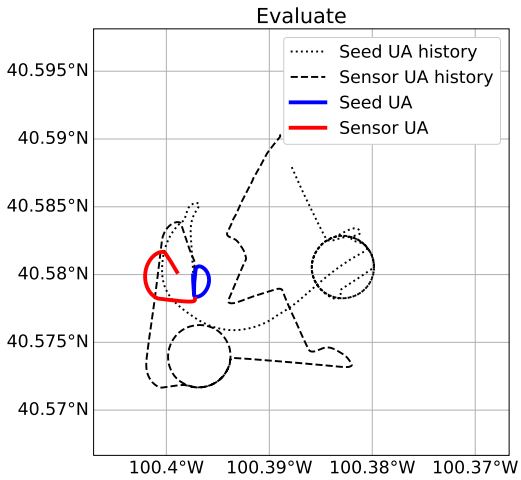

(c) A seeding location is identified, and a seeding maneuver is performed, completing mission #4.

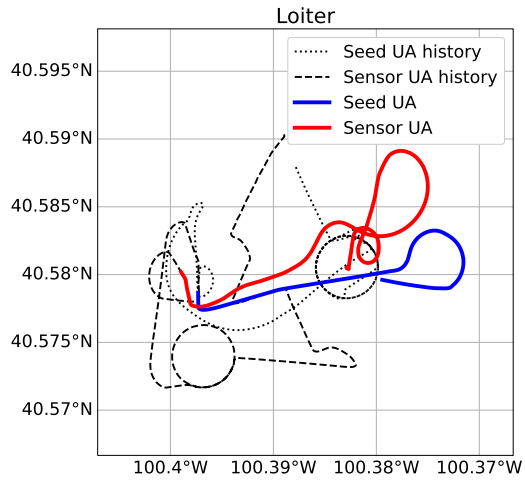

(d) After completing mission #4, both aircraft return to Loiter. With no more impending ROIs to investigate, both aircraft are landed, completing the flight.

Figure 30. Mission #4 completed during Flight #9 on August 28, 2021. Plot titles indicate the state of the Sensor UA.